Tracking an invasion front with environmental DNA

Abigail G. Keller[1], Emily W. Grason[2], P. Sean McDonald[3], Ana Ramón-Laca[4], Ryan P. Kelly[1#]

[1]School of Marine and Environmental Affairs, University of Washington, 3707 Brooklyn Avenue N.E., Seattle, WA 98105, USA

[2]Washington Sea Grant, University of Washington, 3716 Brooklyn Avenue N.E., Seattle, WA 98105, USA

[3]School of Aquatic & Fishery Sciences, University of Washington, 1122 NE Boat St, Seattle, WA 98195, USA

[4]CICOES, University of Washington at Northwest Fisheries Science Center, NOAA, 2725 Montlake Blvd E, Seattle, WA 98112, USA

[#]Corresponding author; rpkelly@uw.edu

Open Research Statement: This manuscript uses novel code, which is provided as supporting information in Data S1, Data S2, Data S3, Data S4, and Data S5. All data and statistical code are available permanently and publicly in Figshare via the following link: https://doi.org/10.6084/m9.figshare.15117102.v2.

Abstract

Data from environmental DNA (eDNA) may revolutionize environmental monitoring and management, providing increased detection sensitivity at reduced cost and survey effort. However, eDNA data are rarely used in decision-making contexts, mainly due to uncertainty around (1) data interpretation and (2) whether and how molecular tools dovetail with existing management efforts. We address these challenges by jointly modeling eDNA detection via qPCR and traditional trap data to estimate the density of invasive European green crab (*Carcinus maenas*), a species where, historically, baited traps have been used for both detection and control. Our analytical framework simultaneously quantifies uncertainty in both detection methods and provides a robust way of integrating different data streams into management processes. Moreover, the joint model makes clear the marginal information benefit of adding eDNA (or any other) additional data type to an existing monitoring program, offering a path to optimizing sampling efforts for species of management interest. Here, we document green crab eDNA beyond the previously known invasion front and find the value of eDNA data dramatically increases with low population densities and low traditional sampling effort, as is often the case at leading-edge locations. We also highlight the detection limits of the molecular assay used in this study, as well as scenarios under which eDNA sampling is unlikely to improve existing management efforts.

Key Words

Bayesian modeling, *Carcinus maenas*, environmental DNA, European green crab, false positive probability, invasion front, invasive species management, N-mixture modeling

Introduction

Since the first documented use of environmental DNA (eDNA) methods for detecting macro-organisms (Ficetola et al., 2008), the fields of conservation and ecology have seen a wave of eDNA studies, with wide ranging applications across a myriad of ecosystems and target taxa (Beng & Corlett, 2020; Bohmann et al., 2014; Deiner et al., 2017; Thomsen & Willerslev, 2015). Techniques such as quantitative polymerase chain reaction (qPCR), digital droplet PCR (ddPCR), and high throughput sequencing (HTS) are increasingly accessible, and can often detect trace amounts of DNA in environmental samples (Jerde, 2019). These molecular techniques yield high-resolution biological information and are particularly useful where traditional monitoring may be infeasible, labor-intensive, or reliant upon diminishing taxonomic expertise (Kelly et al., 2014); in some cases, eDNA assays are more sensitive than traditional sampling methods in detecting rare individuals (Goldberg et al., 2013; Jerde et al., 2011). Together, these attributes make eDNA sampling attractive for detecting rare, cryptic, or elusive aquatic species – and in particular, invasive species.

Early detection and monitoring are key components of successful invasive species management strategies (Lodge et al., 2006), and detection at early stages of establishment has led to eradications of nascent invasions (Anderson, 2005; Wimbush et al., 2009). However, the effort required to detect a species is inversely proportional to its population size (Hayes et al., 2005), and so invasion fronts present a particular management challenge. Historically, cost-effective management strategies have had to balance high survey costs for small populations and high eradication costs if the survey fails to detect an incipient population in the initial stages of invasion (Lodge et al., 2006). Genetic approaches may better detect rare individuals, and thereby lower costs and improve the sensitivity of surveys for small populations, such as those at

invasion fronts (Beauclerc et al., 2019; Harper et al., 2018; Jo et al., 2021; Kuehne et al., 2020; Schütz et al., 2020). However, traditional monitoring methods outperform some eDNA assays (Rose et al., 2019; Ulibarri et al., 2017), underscoring the importance of side-by-side comparisons of detection efficiency.

Despite the advantages of eDNA for early detection of small populations, few examples exist of eDNA methods used to guide decision making. Notable exceptions include the United Kingdom's acceptance of eDNA qPCR results as evidence for the presence of the protected great crested newt, *Triturus cristatus*; there, developers can be prohibited from developing wetlands where there have been positive eDNA detections (Biggs et al., 2015; Natural England, 2017). Perhaps the best example of management-relevant eDNA surveys focuses on the invasive bighead and silver carps (*Hypophthalmichthys* spp.; often referred to jointly in the United States as "bigheaded carp") (Mize et al., 2019), for U.S. Fish and Wildlife Service (Woldt et al., 2020) and U.S. Department of Agriculture (Carim et al., 2016) have protocols that guide field and laboratory eDNA methods, as well as outline recommendations for sampling plans and schedules to be implemented by regional sampling agencies.

Typically, however, methodological development outpaces systematic plans for how to use DNA evidence to support management decisions. Consequently, managers have been slow to adopt eDNA-based approaches in decision making frameworks, (Bohmann et al., 2014; Darling & Mahon, 2011) due to gaps in understanding of the dynamics of eDNA in space and time, as well as the susceptibility of eDNA methods to false negative detections and false positive detections (Darling et al., 2021; Goldberg et al., 2016; O'Donnell et al., 2017; Sepulveda et al., 2020). Although all sampling methods have potential errors, there are many mechanisms for eDNA methods to indicate a false presence, and the fear of a false positive detection is cited as

the primary obstacle to adopting eDNA-based methods in species monitoring (Jerde, 2019). Even though emerging statistical approaches aim to estimate the probability of false positive error (Griffin et al., 2019; Guillera-Arroita et al., 2017), clearly communicating of the meaning of false positive errors – and more generally, uncertainty surrounding the meaning of results – to managers and the public remains challenging (Darling et al., 2021).

Previous reviews highlight the "potential" of eDNA methods to dramatically improve biodiversity assessments and targeted detection of species of concern, as well as the "potential" for unreliability and augmenting of existing uncertainty in environmental management and assessment (Beng & Corlett, 2020; Bohmann et al., 2014; Darling & Mahon, 2011; Yoccoz, 2012). Moving from evaluating the potential value of eDNA data to the practical value of eDNA data requires quantitative and meaningful interpretations of available data (Cristescu & Hebert, 2018; Lacoursière-Roussel & Deiner, 2021), as well as demonstrating the ways in which eDNA does – or does not – complement existing management strategies.

Recent work significantly advances eDNA data interpretation by extending site occupancy modeling methods to estimate species presence and absence using eDNA data (Schmidt et al., 2013). Such models account for imperfect detection when inferring species occupancy and can overcome bias introduced by false negative and false positive detections (Hunter et al., 2015; Lahoz-Monfort et al., 2016; Schmelzle & Kinziger, 2016). Occupancy estimation has become a standard method for modeling species dynamics, monitoring species trends, and informing management (MacKenzie et al., 2002, 2003). The approach has been adapted to accommodate violations of model assumptions (Lele et al., 2012) and survey scenarios where multiple types of observational error occur (McClintock et al., 2010; Miller et al., 2011).

Occupancy models suggest that there are two classes of sites, those that are occupied and those that are not, and these models assume no unmodelled heterogeneity among sites in the probability of detecting a species at a site where it occurs (Royle and Nichols 2003; Altwegg & Nichols, 2019). In reality, variation in local abundance of the species between sites is one important factor that can induce heterogeneity in detection probability with ecological or genetic methods (Royle & Dorazio, 2008), resulting in low estimates of occupancy probability at sites where a species is present but rare. Even for a relatively sensitive assay, a low molecular detection rate can therefore reflect low abundance, rather than low probability of occupancy.

Royle and Nichols (2003) aimed to overcome this limitation by describing a modeling approach that links heterogeneity in abundance to heterogeneity in detection probability, estimating abundance from repeated observations of a species. This heterogeneous detection probability model provides a framework for estimating species density based on abundance-induced variation in detection probability with eDNA methods (Royle & Nichols, 2003). Building on this framework, we jointly model observations from both traditional and eDNA monitoring methods to estimate local species density. The joint model aids management decisions by informing interpretation of molecular detections, the most appropriate use of eDNA sampling efforts, and the relative sensitivities of molecular and traditional sampling methods.

We apply the joint model to eDNA detection data of European green crab, *Carcinus maenas*, in Washington State. Green crab causes massive ecological and economic damage in its invaded range; for example, the species has caused the collapses of the soft-shell clam industry in Maine (Glude, 1955; Tan & Beal, 2015). Green crab was first detected in Washington waters in 1998, after warm El Niño-Southern Oscillation (ENSO) currents spread larvae of California populations up to British Columbia, Canada (Behrens Yamada & Hunt, 2000), and the species is

now classified as a deleterious species in Washington State because of perceived risks to coastal resources (Grason et al., 2018). Washington Department of Fish and Wildlife (WDFW), United States Fish and Wildlife Service (USFWS), Washington Sea Grant, several sovereign tribal nations, and other concerned citizens have subsequently coordinated to surveil and manage green crab along the nearly 3,000 km of Washington's inland shoreline.

Traditionally, crab traps have provided much of the quantitative information about the position of the green crab's invasion front in Washington, and the State invests heavily in deploying traps throughout likely invasion pathways. Here, we couple this existing dataset with qPCR data using a recently developed assay for green crab (Roux et al., 2020), derived from water samples collected throughout the region. We combine these data streams to estimate the density of green crab across the study sites using the joint model, and we highlight changes in the precision of these estimates in the joint model vs. a model that uses only traditional trapping data; the difference between the two is the marginal information benefit of eDNA for this particular management purpose. This modeling framework offers a path to improve interpretation of eDNA data, as well as identify the scenarios under which eDNA sampling will most likely improve existing management efforts.

Methods

i. Joint model description

We model traditional trap data and eDNA qPCR detections jointly, linking the two through a shared species density at each sampling site (Data S1).

Traditional monitoring methods – here, trapping – relate repeated capture rates to an underlying species density. Since previous work analyzing green crab capture in traps found

patchy distribution, with significant local-scale variation within a site (Bergshoeff et al., 2019), we modeled the capture process using a negative binomial distribution to account for overdispersion. We also conducted a leave-one-out cross-validation approach to evaluate the relative predictive accuracy of distribution choices for modeling the capture process based on the observed data (Vehtari et al., 2017) (Appendix S1, Data S2). The observed count, Y, of a species at site *i* and trap sample *k* is drawn from a negative binomial distribution with a mean species density, μ_i, and an overdispersion parameter, Φ (*Eq. 1*).

$$Y_{i,k} \sim NegBinomial\left(\mu_{i,}\Phi\right) \quad (1)$$

Guided by the principle that the probability of detection with qPCR increases as the underlying species density increases, we describe the probability of a true molecular detection, p_{11}, at site *i* as a saturating function of species density, μ_i, and scaling coefficient, β (*Eq. 2*).

$$p_{11,i} = \frac{\mu_i}{\mu_i + \beta} \quad (2)$$

Recognizing the susceptibility of eDNA methods to false positive errors (Roussel et al., 2015; Sepulveda, Nelson, et al., 2020), we incorporate a false positive probability, p_{10}, that represents two sources of false positive detections: (1) presence of target DNA in the sample but absence of target organism at the associated site, arising from processes like laboratory contamination or transportation of target cells from far away locations, and (2) absence of target DNA in the sample but a positive molecular detection, arising from non-specific amplification.

The false positive probability, p_{10}, contributes to the overall molecular detection probability, p, at site *i* (*Eq. 3*; p is bounded between 0 and 1).

$$p_i = p_{10} + p_{11,i} \quad (3)$$

We estimate these parameters through repeated molecular observations at each site using a species-specific quantitative PCR (qPCR) assay (Roux et al., 2020). Many applications of qPCR are interpreted as molecular binary indicators of detection (1) or nondetection (0) (Guillera-Arroita et al., 2017; Orzechowski et al., 2019; Schmidt et al., 2013), and the binomial distribution is suitable for modeling "successes" in a given number of trials (Hobbs & Hooten, 2015). The number of positive qPCR detections, K, out of the number of trials, N, in water sample *j* at site *i* is drawn from a binomial distribution, with a probability of success on a single trial, p_i (*Eq. 4*). Due to the hierarchical qPCR data structure, where qPCR triplicates are nested within water bottles within sites, we also provide a hierarchical version of the model that accounts for membership of qPCR replicates within nested groups (Appendix S2, Data S3). We present a simpler model here.

$$K_{i,j} \sim Binomial\left(N_{i,j},\ p_i\right) \quad (4)$$

We implement the model in a Bayesian framework, in which the posterior probability of the model parameters (given observed data) is product of the individual likelihood functions at site, *i*, water sample, *j*, and trap sample, *k*, as well as the prior probabilities (*Eq. 5*). A gamma distribution was used as the prior distribution for parameters μ_i, Φ, and β because of its

suitability for continuous, non-negative random variables. These priors allow us to incorporate existing information into the analysis and help to make the parameters identifiable.

$$[\mu_i, \phi, \beta, p_{10}] \propto \prod_{i=1}^{n}\prod_{j=1}^{m}\prod_{k=1}^{p} NegBinomial(Y_{i,k} \mid \mu_i, \phi) \times Binomial(N_{i,j}, K_{i,j} \mid p_{10}, \mu_i, \beta) \times Gamma(\mu_i \mid \alpha_\mu, \beta_\mu) \times Gamma(\phi \mid \alpha_\phi, \beta_\phi) \times Normal(p_{10} \mid \mu_{p10}, \sigma^2_{p10}) \times Gamma(\beta \mid \alpha_\beta, \beta_\beta) \quad (5)$$

We specified the model within Stan, a probabilistic programming language written in C++ that implements full Bayesian statistical inference using Markov chain Monte Carlo, and used the package 'rstan' (version 2.21.2) as an interface to the R (version 4.1.1) software environment (Carpenter et al., 2017; Guo et al., 2020; R Development Core Team, 2021).

ii. Green crab eDNA data collection

eDNA field sampling

Twenty sites with varying known presence and abundance of green crab were chosen for eDNA sampling (Figure 1, Appendix S3: Figure S1), and given the time scale of the sampling effort, all sites were distinct with relation to green crab movement. At each site we collected five 500 mL surface water samples 1-5 meters apart. All sampling equipment was soaked in 10% bleach between sites and thoroughly rinsed in deionized water to prevent cross-contamination. Water samples were placed on ice and vacuum-filtered onto a cellulose acetate filter (47 mm diameter, 0.45 µm pore size) within four hours of collection, except for samples from the KVI site, where samples were stored at 4°C and filtered 24 hours after collection due to vacuum equipment malfunction. Filters were preserved in 900 µL of Longmire buffer (Longmire et al.,

1997; Renshaw et al., 2015) and stored at -80°C for 1-3 weeks before DNA extraction. We collected a total of 100 eDNA water samples.

eDNA sample processing

We extracted DNA from filters using a phenol:chloroform:isoamyl alcohol protocol (modified from (Renshaw et al., 2015) and described in (Gallego et al., 2020)). One negative control (900 µL of Longmire buffer) was extracted during each set of DNA extractions (n = 3 total). We quantified DNA purity on a spectrophotometer (Nanodrop, Thermo Scientific, Inc.) and DNA concentration on a fluorometer (Qubit, Invitrogen, Inc.) to determine DNA extraction success.

Each eDNA extract was amplified by qPCR using a *C. maenas*-specific assay developed by Roux et al. (2020) that targets a 148 bp fragment of the cytochrome c oxidase 1 (CO1) region. Three qPCR replicates were run for each eDNA extract in 25 µL reactions following Roux et al. (2020), but we modified the protocol to use TaqPath™ ProAmp™ Master Mix due to its relatively high tolerance of inhibitors (Applied Biosystems, A30865). Three negative PCR controls containing 2 µL of molecular grade water were included in each reaction, and each extraction negative control was run in triplicate. All qPCR reactions were performed on Applied Biosystems StepOnePlus Real-Time PCR System an analyzed with StepOne Software v2.3. Any DNA template passing the fluorescence threshold in fewer than 38 cycles was considered a positive amplification, since 38 Ct is the average Ct value corresponding to the assay's limit of detection with 50% chance of detection (Roux et al., 2020). The identity of 13 qPCR products from four sites were confirmed through unidirectional Sanger sequencing with the forward

primer; all sequences were unambiguously *C. maenas*, and no other crabs from the same taxonomic family are present in the region (Appendix S4: Table S1).

In addition to the 20 sites sampled concurrently with trapping efforts, eDNA samples from seven sites in Skagit Bay, WA were analyzed using the same sampling, DNA extraction, and qPCR procedures (Appendix S4: Table S2). These sites were characterized as unsuitable for green crab based on expert opinion and were included as sites of unambiguous crab absence to inform the prior on the estimated probability of a false positive molecular detection (p_{10}). Four water samples at each of the seven sites were processed at an independent laboratory facility (NOAA Northwest Fisheries Science Center), where each water sample underwent triplicate qPCR reactions, alongside nine no-template negative controls and three field blank negative controls.

Inhibition Testing

To ensure negative qPCR detections were not systematically due to PCR inhibition, we measured potential inhibition occurrence by analyzing the quantification threshold (Ct) deviation of a spiked internal positive control. A synthetic (gBlock) positive control was spiked into samples with no positive amplifications (Integrated DNA Technologies, Inc.). The double-stranded 200 bp gBlock oligonucleotide contained green crab-specific primer and probe sequences, with three modified bases between the forward primer and probe and two modified bases between the probe and reverse primer to identify contamination at the amplification step. For sites where all eDNA replicates previously tested negative for green crab, we subsequently tested one eDNA sample per site for inhibition. For sites where some but not all eDNA replicates tested negative for green crab, each previously negative eDNA sample was tested for inhibition.

Each qPCR reaction used 1 µL of environmental DNA extract and 1 µL of the gBlock positive control at a final reaction concentration of 0.20 gBlock copies/µL. Three qPCR replicates containing 1 µL of the gBlock positive control (without eDNA extract) at a final reaction concentration of 0.20 copies/µL was also included in the reaction. Inhibition occurrence was measured as the difference in Ct, ΔCt, between the Ct value of the spiked eDNA sample and the mean of the three positive gBlock controls ($Ct_{sample} - Ct_{control}$) (Volkmann et al., 2007). We conservatively considered a ΔCt greater than two cycles to be evidence of inhibition, considering that three cycles – as is common in the literature (Hinlo et al., 2017) -- is almost one order of magnitude difference in concentration in an efficient reaction. Each DNA sample underwent 1-3 passes through a OneStep PCR Inhibitor Removal spin column (Zymo Research Corp.) until inhibition occurrence was not detected (Appendix S4: Table S3).

iii. Green crab trapping data

The Washington State Department of Fish and Wildlife, Washington Sea Grant, U.S Department of Fish and Wildlife, and Jamestown S'Klallam Tribe provided data from baited traps from a larger green crab monitoring program. Traps were set for an overnight soak and collected within 24 hours of placement; any trapped green crabs were counted and subsequently removed from the system. Trap types included in the dataset were Gee-brand galvanized steel minnow trap (5.08 cm opening, 0.635 cm mesh) and the square Fukui fish trap (1.27 cm mesh), which have similar catchability for green crab and mechanisms of trapping.

The sampling sites vary with respect to known green crab presence, abundance, and trapping effort (Appendix S3: Figure S1). Trapping effort ranged from three to 420 traps set over the selected trapping period, and water samples were collected two weeks before or after trap

collection, with the exception of the Stackpole site (STA) (Appendix S3: Figure S2). At STA, only three traps were set during the sampling period, and no green crabs were recovered. To reflect the relatively high density of green crab determined through previous, greater trapping efforts, trapping data at STA collected eight weeks before eDNA sampling were included in the dataset (Appendix S3: Figure S2). Despite trapped crabs being removed from the system, our analysis assumed that these removals did not substantially change the relative densities of green crab at the sampled sites over the sampling period (Appendix S3: Figure S2).

iv. Joint model application: green crab density estimates

We fit the joint model to the qPCR and trap observations using weakly informative priors for all parameters except the false positive rate of detection, p_{10}, for which we used an informative prior from negative control data in Roux et al. (2020) and the eDNA samples from sites characterized *a priori* as unsuitable for green crab. We set the p_{10} prior at beta(1,28), such that the false positive detection probability is likely less than 0.036 ($P(p_{10} < 0.036) = 0.64$). For ease of model-fitting in Stan, we moved p_{10} to a log scale, and used moment-matching to convert the beta prior into a lognormal distribution (Hobbs & Hooten, 2015). To reflect prior knowledge of the presence of green crab at each site beyond the information provided in the trap data, different hyperparameters were used for the prior distributions for μ based on green crab recovery at the sampled sites from 2017-2021 (Appendix S4: Table S2). The prior distribution for μ at sites with a history of trapped green crab was $\mu_{crab} \sim gamma(0.25, 0.25)$, and the prior distribution for μ at sites without a history of trapped green crab was $\mu_{nocrab} \sim gamma(0.05, 0.05)$. Priors for the other model parameters were as follows: $\beta \sim gamma(2, 1)$ and $\Phi \sim gamma(0.25, 0.25)$.

We ran the joint model via 'rstan', with a step size of 0.5 and 4 chains with 500 warm-up and 2,500 sampling iterations per chain, and we checked for model convergence through the R-hat convergence diagnostic and by visually examining the resulting autocorrelation plots and chain mixture in the trace plots using the package 'shinystan' (Gabry et al., 2018). For comparison, we ran a trap-only model (*Eq. 1*) in the same way.

As crab density decreases, the probability of a true positive molecular detection decreases, and at very low crab densities, the probability of a false positive detection, p_{10}, is higher than the associated true positive detection, p_{11}. Here, we defined the crab density threshold at which a detection is equally likely to be true or false ($p_{10} = p_{11}$) as the critical crab density, $\mu_{critical}$. This value was calculated using the model's posterior distributions of estimated parameters, p_{10} and β, and the relationship between μ and p_{11} defined in *Eq. 2*.

v. Robustness Assessments

A sensitivity analysis was conducted to ascertain the sensitivity of the model's inferences to the specification of the false positive probability, p_{10}, prior distribution. The joint model was refit using a set value for p_{10} under a range of values (0.005-0.055), and all other parameters (β, Φ, μ_i) were estimated. All refitted models were run with a step size of 0.5 and 4 chains with 500 warm-up and 2,500 sampling iterations per chain and were checked for model convergence.

We also examined the effect priors had on our inferences by conducting a data cloning procedure described by Lele et al. using the package 'dclone' (version 2.3-0) (Data S1) (Lele et al., 2007; Solymos, 2019). We replicated the qPCR and trapping datasets (n=10) for each sampled site and used these copies as data input in our model to swamp the posterior distribution, which subsequently minimizes the influence of the prior distributions and yields

estimator outputs that are asymptotically equivalent to maximum likelihood estimators (Lele et al., 2007). We evaluated the influence of the prior distributions on our model's inferences by comparing data cloning parameter estimates to our Bayesian parameter estimates.

We then compared our model's inferences to parameter estimates derived from an occupancy modeling framework. We estimated occupancy parameters using the qPCR detection data and the R package, 'msocc' (version 1.1.0), which implements a Gibbs sampler to fit Bayesian multi-scale occupancy models (Data S1) (Stratton et al., 2020). The occupancy model was run with 11000 total MCMC iterations (1000 burn-in iterations), and site-specific sample-level probabilities of occupancy, θ_i, and site-specific replicate-level probabilities of occupancy, p_i, were estimated. Replicate-level probabilities of occupancy, $p_{i,occupancy}$, were compared to the overall probabilities of molecular detection, $p_{i,joint}$, from the joint model, and a linear regression was fit to model the relationship between $p_{i,occupancy}$ and $p_{i,joint}$ using the lm() function in R.

vi. Evaluation of eDNA data's marginal benefit

As information increases, uncertainty decreases. We therefore considered a reduction in uncertainty around green crab density estimates as a measure of the marginal value of eDNA data, relative to the baseline information contained in trap data alone. We quantified precision in the estimates of green crab density, μ_i, using a coefficient of variation (CV; the standard deviation of the parameter estimate divided by the mean), to facilitate comparisons of variability across green crab densities of differing orders of magnitude (Abdi, 2010). We calculated the change in precision (ΔCV) in the parameter estimates in the joint model vs. trap-only model as $CV_{trap} - CV_{joint}$, and we analyzed this change in precision as a function of trapping effort. qPCR

effort remained constant throughout data collection. We captured the resulting exponential trend line in the relationship between ΔCV and trapping effort using the method of least squares.

To evaluate the sensitivity of eDNA vs. trap sampling, we estimated the sampling effort necessary to detect a green crab with 90% confidence. A detection refers to either capturing at least one green crab in a trap or producing at least one true positive qPCR amplification. For trap sampling, we calculated the minimum number of traps necessary to be 90% confident that at least one crab would be caught (*Eq. 1*, given a non-zero expected number of crabs/trap, μ, and the model's median estimate for dispersion parameter, Φ). For eDNA sampling, we defined effort as the number of unique water samples, each having triplicate qPCR. We calculated the minimum number of water samples, *E*, necessary to detect the true presence of crab with at least 90% confidence as binomial(E*N, p11), where *N*=3. p11 was defined as in *Eq. 2* and depends upon the underlying true number of crabs/trap, μ, and the model's median estimate for parameter β. Both sampling type analyses were conducted under a range of crab densities, from median $\mu_{critical}$ – 3.0 crabs/trap.

vii. Simulation study

We simulated the precision and accuracy of green crab density estimates as a function of sampling strategy, given a range of green crab trapping efforts and true species densities. Both qPCR data and green crab trap count data were simulated for each of nine green crab densities (0, 0.02, 0.05, 0.1, 0.15, 0.25, 0.5, 1, 3 crabs/trap (μ_{sim})) and eleven trapping efforts (3, 4, 5, 7, 10, 12, 15, 20, 30, 40, 60 traps), for a total of 99 scenarios. The eDNA sampling effort was held constant at five biological replicates and three technical replicates for all simulated scenarios. Each scenario made up a different site, i_{sim}, in the overall simulated dataset, and we simulated

each dataset 50 times to capture stochasticity. These scenarios represented the range of green crab densities and trapping efforts observed in this study.

We then used the simulated datasets to estimate the underlying green crab density, μ_{sim}, at each simulated site, i_{sim}, with both the joint and trap-only models. Only parameter μ_{sim} for each simulated site was estimated by the two models, and parameters p_{10}, β, and Φ were set at the joint model's median estimate derived from collected data. A prior distribution for μ of gamma(0.05, 0.05) was used at all simulated sites, and each model was run with 4 chains of 500 warm-up iterations and 2,500 sampling iterations (Data S4). We calculated the mean change in precision (ΔCV) of the 50 simulation replicates at each simulated site to determine the effect of trapping effort and underlying crab density on changes in estimated crab density precision. We calculated model accuracy for each simulation scenario as the proportion of simulation replicates that yielded a 90% credibility interval containing the true density, μ_{sim}.

Results

i. Green crab genetic and traditional monitoring data collection

We detected at least one positive amplification at 13 sites, (1 – 15 amplifications out of 15 total qPCR replicates per site; five biological replicates x three technical replicates per site; Appendix S4: Table S3). In a total of 1274 trap observations (3 - 420 traps set over the sampling period; Appendix S3: Figure S2), green crabs were trapped at nine of the 20 sampled sites over the sampling period (mean crabs/trap 0 – 6.04). All nine of these sites had positive eDNA detections, while four additional sites yielded at least one positive eDNA detection where no green crabs were trapped over the sampling period (Figure 1). At two of these four additional sites, green crabs were recovered in traps over a longer time horizon (2017-2021) than the extent

of the sampling period (Appendix S4: Table S2). All samples collected at sites characterized as unsuitable for green crab produced negative qPCR results, and all no-template (negative) qPCR controls and DNA extraction blanks produced negative qPCR results.

ii. Detection of green crab eDNA beyond known invasion front

Both the joint and trap-only models yielded an R-hat of one for all estimated parameters and produced well-mixed chains and low serial autocorrelation, indicating model convergence. The median calculated critical crab density, $\mu_{critical}$, or threshold where the true positive probability of molecular detection equals the false positive probability of molecular detection ($p_{10} = p_{11}$) was 0.056 crabs/trap (0.010, 0.12 90%CrI).

The joint model estimated a relatively high green crab density in a location beyond the previously known invasion front (Figure 2) and provided well-constrained estimates of parameter values, including the false positive rate (p_{10} = 0.022, (0.0095, 0.048 90%CrI); Table 1). Green crab eDNA was detected on Vashon Island, more than 60 km south of the southernmost visual observations of the species (Figure 2). The median estimated green crab density at the Raab's Lagoon (RAA) site on Vashon Island was 0.16 crabs/trap (4.0e-61, 0.61 90%CrI) (Figure 3, Appendix S4: Table S4). The probability that the green crab density at Raab's Lagoon (RAA) was greater than the median $\mu_{critical}$, 0.056 crabs/trap, was 0.64. This relatively high density of green crab was similar to density estimates at sites in Whatcom region, where historically green crabs have been recovered in traps under high trapping efforts (estimated densities 0.065 – 0.59 crabs/trap, Appendix S4: Table S4).

The concurrent eDNA and trap sampling meaningfully constrained the lower limit of eDNA sampling's sensitivity relative to trap sampling. At Graveyard Spit Channel, the eDNA

samples yielded no positive molecular detections, and no green crabs were trapped out of the 86 traps set during the sampling period. The estimated median green crab density at this site was low (0.00049 crabs/trap; 2.4e-18, 0.0079 90%CrI). However, in 2020, 1369 traps were set, and three green crabs were recovered (0.002 crabs/trap), and in April 2021, three more crabs were recovered at this site, indicating that it is nearly certain that crabs were present in the channel during the time of sampling but not detected by eDNA sampling; this appears to be a false negative result.

Three sampled sites—Indian Island (IND), Jimmycomelately creek (JIM), and KVI Beach (KVI)—yielded one positive molecular detection, yet their median estimated crab densities were below $\mu_{critical}$, or the crab density at which the false positive probability of detection equals the true positive probability of detection, given the estimated crab density (Appendix S4: Table S4). The probability that the crab densities were greater than the median $\mu_{critical}$ was 0.35, 0.017, and 0.096 for IND, JIM, and KVI, respectively. Given the estimated crab densities at these sites, these molecular detections were as likely to be a false positive detection than a true positive detection. One sampled site, Jimmycomelately creek (JIM), in the Central Sound produced one positive qPCR detection, yet the 43 traps set over the sampling period recovered zero green crab individuals. During 2020, no green crabs were recovered in traps, but in July 2021, nine months after eDNA sampling, five adult green crabs were recovered in in a neighboring channel to the site sampled for eDNA.

iii. Robustness Assessments

The model refitting procedure using set values for the false positive probability p_{10} (p_{10} = 0.05-0.55) indicated that some parameter estimates were sensitive to p_{10}. Among the four sites

with at least one positive eDNA detection and no crabs trapped over the sampling period (RAA, IND, KVI, JIM), all four μ estimates were sensitive to the value set for p_{10} during model refitting (Appendix S3: Figure S3a, Figure S3c). At these sites, lower values of p_{10} yielded higher estimates of μ, and this effect was strongest for sites with a low trapping effort (RAA, IND, KVI) (Appendix S3: Figure S3a, Figure S3c). All other μ estimates at the remaining 16 sites were insensitive to the set value of p_{10} (Appendix S3: Figure S3d). As expected with a lower p_{10} and subsequently a more sensitive assay, lower set values of p_{10} yielded lower estimates of the scaling parameter, β (Appendix S3: Figure S3b).

For the data cloning procedure, all parameter maximum likelihood estimates were within the 90% credibility intervals estimated by the Bayesian model. The median maximum likelihood estimates of μ (μ_{MLE}) were nearly identical to the median Bayesian estimates of μ (μ_{Bayes}), although the median μ_{MLE} was slightly higher than the median μ_{Bayes} at sites with a lower trapping effort (Appendix S3: Figure S4). The median maximum likelihood estimate of Φ was 0.96, which was nearly identical to the median Bayesian estimate of Φ (0.94) (Table 1). The median maximum likelihood estimate of β was 2.3, and the median maximum likelihood estimate of p_{10} was 0.012. Both median MLE estimates of β and p_{10} were lower than their respective median Bayesian parameter estimates, yet the median MLE estimates were inside the Bayesian 90% credibility intervals (Table 1).

The joint model's inferences were also consistent with parameters estimated from an occupancy modeling framework. The site-specific replicate-level probabilities of occupancy, $p_{i,occupancy}$, were consistent with site-specific molecular probabilities of detection, $p_{i,joint}$, from the joint model (Appendix S3: Figure S5). A linear regression between the two parameters indicated that 71.8% of variation in $p_{i,occupancy}$ was explained by $p_{i,joint}$ (F-statistic: 45.9, p-value: 2.40e-6).

476

477 ***iv. Quantifying uncertainty to find the value of eDNA information***

478 At sites with lower trapping effort, adding eDNA data narrowed the credibility intervals
479 for estimated crab density, relative to a model using only trapping data. Moreover, the leading
480 edge of an invasion, like the Central and South Sound, often features low densities of the
481 invading species; here, the combination of eDNA and trapping data vastly reduced the
482 uncertainty associated with low trapping effort in these cases (Figure 4). As the trapping effort
483 decreased, the marginal benefit (ΔCV) of eDNA data increased exponentially (Figure 4),
484 dramatically increasing the precision of green crab density estimates at sites along the invasion
485 front and at sites characterized by low trapping efforts.

486 To identify the relative sensitivities of the two sampling methods, we determined the
487 sampling effort necessary to detect a green crab with 90% confidence, given the joint model's
488 estimated parameters. This sampling effort was calculated for a range of simulated crab
489 densities, from 0.056 crabs/trap (median estimated $\mu_{critical}$) to 3.0 crabs/trap. The detection
490 sensitivity -- the probability of capturing at least one crab in one trap or the probability of one
491 true positive qPCR amplification in triplicate trials -- was higher for eDNA sampling than for
492 trap sampling, suggesting that the information provided by one water bottle is slightly greater
493 than the information provided by one trap (Figure 5).

494

495 ***v. eDNA's greatest marginal benefit at low species densities and trapping effort***

496 Simulations further indicated that the marginal benefit of eDNA data, measured as ΔCV,
497 increased as trapping effort decreased for all simulated densities of green crab (Figure 6).
498 Importantly, these information benefits tended to be highest at true crab densities (μ_{sim}) in the

499 range 0.05 – 0.50 crabs/trap, and the information benefit decreased at crab densities higher and
500 lower than this range (Figure 6).

501 Both the joint and trap-only models produced accurate estimates of green crab density in
502 a diverse set of simulations. For scenarios where $\mu_{sim} > 0$, 100% of simulation replicates yielded
503 90% credibility intervals of density estimates that contained the true green crab density, μ_{sim}. For
504 scenarios where $\mu_{sim} = 0$, no simulation replicates yielded 90% credibility intervals of density
505 estimates that contained the true green crab density, μ_{sim}.

506

507 ## Discussion

508 Many management and policy decisions have prominent economic and social
509 consequences, particularly surrounding invasive or endangered species, which often occur at low
510 densities. Finding the leading edge of an invasion front can correspondingly require government
511 agencies and others to engage in high-cost sampling that nevertheless has little power to detect
512 rare individuals. As eDNA comes to the forefront as a routine sampling technique that can
513 ameliorate some of these difficulties, it is important to quantify the value of this new data stream
514 and to adequately characterize the uncertainty associated with all kinds of environmental
515 sampling. By jointly modeling eDNA and traditional (trap) data for the invasive European green
516 crab, we (1) estimate the abundance of the species at its leading edge of invasion, (2) quantify
517 uncertainty in both detection methods and show the marginal information benefit of an eDNA
518 data stream, and (3) offer a framework for integrating eDNA into existing data streams and
519 survey programs.

520

521 *Improving interpretation of eDNA data*

Our quantitative approach builds upon previous work adapting occupancy modeling approaches to facilitate eDNA data interpretation (Griffin et al., 2019; Lahoz-Monfort et al., 2016; Pilliod et al., 2013; Schmidt et al., 2013). These previous approaches suggest that there are two classes of sites—those that are occupied and those that are not—and crucially, that the probability of detecting a species is constant within a given ecological context. This assumption can be insufficient in the context of eDNA surveys, where local abundance can induce heterogeneity in detection probability (Altwegg & Nichols, 2019; Royle & Nichols, 2003; Royle & Dorazio, 2008). The joint model presented here uses the heterogeneity in molecular detection probability to estimate species density, rather than occupancy, and operates under the assumption that the probability of a true detection increases as species density increases.

The joint model uses observations from two sampling methods, each generated independently from a shared underlying species density. The two data streams inform one another: the combined likelihood borrows strength from the sites with greater trapping effort over the sampling period to infer detection biases across all locations and to inform species density at data-limited sites. The model also reveals the relative sensitivities of the two sampling methods and the relative information contributions of eDNA data at varying trap sampling efforts.

In practical application, environmental factors including flow rates, turbulence, temperature, water chemistry, and UV light can affect the dilution, persistence, and strength of an eDNA signal (Andruszkiewicz et al., 2017; Barnes & Turner, 2016; Deiner & Altermatt, 2014; Sansom & Sassoubre, 2017). Quantitatively modeling eDNA detections and integrating traditional and new sampling approaches helps to mitigate this challenge by capturing uncertainty in how eDNA detections arise from true species presence and density.

To overcome challenges with parameter identifiability typical of hierarchical models of eDNA data (Griffin et al., 2019; Guillera-Arroita et al., 2017), the model uses a Bayesian framework and sets plausible bounds on the false positive probability as prior information. Recognizing the tendency for Bayesian priors to induce undue influence on the model's inferences (Cressie et al., 2009; Lele & Dennis, 2009), we conduct robustness assessments to investigate the effect of prior assumptions. We find that our inferences are largely robust to prior specification (Appendix S3: Figure S3 and Figure S4); although at certain sites with a low trapping effort, there is not enough information in the data to limit the influence of the specified false positive probability prior (Appendix S3: Figure S3).

Importantly, the joint model's results can aid appropriate management responses after a molecular detection. In management contexts, positive eDNA detections are commonly used to prompt non-molecular sampling for corroboration (Sepulveda et al., 2020), as shown in the Great Lakes invasive carp eDNA surveillance program (Woldt et al., 2020). However, after a positive eDNA detection, managers must decide how intense (and therefore expensive) the management response must be, and it is often difficult or impossible to confirm a species' absence with traditional methods (Morrison et al., 2007; Russell et al., 2017). Quantifying uncertainty for any given detection method encourages agencies to explicitly set tolerable risk levels for the presence of a target species.

The results of the joint model offer a framework for inferring a species density threshold, $\mu_{critical}$, at which a molecular detection is as likely to be a false positive detection as a true positive detection. This value provides an opportunity to investigate the probability that an eDNA detection reflects the true presence of a species. For example, two sites yielded one positive qPCR detection each, yet the median estimated crab densities are very near zero (0.0013

and 6.5e-7 crabs/trap at Jimmycomelately creek (JIM) and KVI Beach (KVI), respectively). Given the combination of molecular and trapping data in hand, these detections are as likely to be false positives than true positives. Further detections by either method would change this interpretation, but the ability to quantify uncertainty in this way is valuable.

Quantifying the practical value of eDNA information

Our framework offers a way to fold genetic surveys into existing management practices, therefore moving the contribution of eDNA data to management practices from "potential" value to practical value. For the specific example of the green crab assay, the marginal benefit of eDNA data – measured as increases in the precision of species density estimates upon the addition of eDNA data – is highest at sites with low trapping effort, and this information benefit increases exponentially as traditional trapping effort decreases (Figure 4, Figure 6). Thus data-limited applications particularly stand to gain from molecular surveys.

Simulations identify a parameter space, or a combination of true green crab density and existing trapping effort, where the marginal benefit of eDNA information is highest. These simulations suggest that eDNA sampling is most useful at low trapping efforts and a green crab density of about 0.05 – 0.50 crabs/trap, a sampling combination in which a true molecular detection is likely, and a detection through baited trapping is unlikely. Importantly, as the true green crab density falls below about 0.05 crabs/trap (where the true-detection rate (p_{11}) falls below the false-detection rate (p_{10})), the information benefit of eDNA data decreases. Previous work faces similar challenges in detecting green crab eDNA at low densities with existing molecular assays, and suggested a different assay was more sensitive during green crab spawning periods (Crane et al., 2021).

Therefore, the joint model not only indicates where the marginal benefit of eDNA sampling is highest, but also where marginal benefit of eDNA is negligible, which is valuable information for allocating limited monitoring resources. We find eDNA sampling is unlikely to improve management at locations with high trapping effort or a high species density (Figure 4, Figure 6) – situations in which managers essentially already have the information they seek. For example, eDNA samples were collected in Dungeness National Wildlife Refuge, an area rich in marine life that contains one of the world's longest sand spits. The watershed in this area is also home of the Jamestown S'Klallam Tribe, providing abundant resources from its tidelands and marine waters (Jamestown S'Klallam Tribe, 2007). U.S. Department of Fish and Wildlife implements an intense removal trapping procedure in the national refuge. In 2020 in Graveyard Spit Channel (GSC), 1369 traps were set, and three green crabs were recovered. The combination of high trapping effort and inferred crab densities well below $\mu_{critical}$ means eDNA sampling would be unlikely to improve the existing survey estimates at this site.

The veracity of negative results are often of equal importance as confirmation of positive detections, and eDNA sampling has previously been used in species eradication campaigns (Carim et al., 2020; Davison et al., 2019; Larson et al., 2020). However, the sensitivity of the assay we tested here illustrates a case in which the similar rates of detection between traditional and molecular sampling mean that it is difficult to confirm a species' absence with either method (Morrison et al., 2007; Russell et al., 2017).

Although costs of eDNA-based surveys tend to compare favorably with those of traditional capture-based methods (Biggs et al., 2015; Sigsgaard et al., 2015), future work should identify the survey regime that maximizes detection probability under a fixed budget. Previous cost-efficiency analyses find that eDNA is less cost-efficient at low sample numbers, since costs

associated with initial investments in reagents and supplies for laboratory analysis are high (Smart et al., 2016). However, since traditional sampling requires repeat visits and more time- and labor-intensive sampling effort, eDNA sampling has lower field labor and transportation costs and can become more cost-effective compared to traditional sampling when examining a large number of sites (Khalsa et al., 2020). Such cost comparisons are critical when identifying the optimal allocation of survey effort to maximize detection, and future cost-efficiency inquiries should consider the role of site-specific characteristics that affect the relative costs of sampling methods.

Increasing certainty at the green crab's invasion front

By contrast, sites with low trapping effort are likely to benefit from the additional information eDNA offers. In the context of green crab, the most notable example of eDNA data's value at the invasion front is the estimation of a relatively high green crab density at a site well beyond green crab's previously known distribution (Figure 2, Figure 3, Appendix S4: Table S4). By interpreting the pattern of eDNA signals, the joint model indicates green crab eDNA presence with relatively high certainty at Raab's Lagoon (RAA) on Vashon Island, suggesting that the local species density is perhaps low and previously undetectable using traditional monitoring methods implemented at a low effort. We estimate the green crab density at Raab's Lagoon – one of the sites beyond the previously known invasion front – to be 0.16 crabs/trap (4.0e-61, 0.61 90%CrI). The probability that the green crab density is greater than the median $\mu_{critical}$, or the crab density at which the associated true probability of detection equals the estimated false positive probability, is 0.64 (Figure 2, Appendix S4: Table S4). This finding is consistent with studies showing that sufficient eDNA sampling applied across large geographic

areas can reveal unexpected patterns and new occurrences of species missed by traditional approaches (Mckelvey et al., 2016; Tucker et al., 2016), and the Bayesian modeling framework allows these statements of new occurrences to be tempered by quantified uncertainty (Hobbs & Hooten, 2015). However, the model treats molecular detections and trapped adults as conceptually equivalent, with a joint estimate of species "density" in units of crabs per trap. This is a somewhat imprecise description insofar as molecular detections potentially include larval and dead individuals. Depending upon management priorities, detections of larval or dead individuals may (or may not) rise to the level of importance of live adult detections. Indeed, results of trapping at RAA and KVI in July 2021 suggest that these molecular detections may have been larvae, and to date, no adults have been captured at RAA, KVI, or neighboring sites in the South Sound through trapping efforts by WSG Crab Team, WDFW, and partners.

False Positives and False Negatives

The fear of false positive detections is often cited as the primary hurdle for adopting eDNA approaches for species monitoring (Jerde, 2019). However, the term "false positive" can be misleading in the eDNA context (Darling et al., 2021): different mechanisms contribute to false positive errors, and we can distinguish between errant detection in an individual sample vs. errant detection at an unoccupied site (Chambert et al., 2015; Darling et al., 2021; Guillera-Arroita et al., 2017). Our model explicitly estimates a molecular false positive probability, which incorporates both the probability of a false positive sample and the probability of a false positive site through information included in the parameter's prior distribution and unambiguous presence sites with a high trapping intensity. In this study, however, field negative controls (clean water collected using the same protocol and equipment as field samples) were not

collected at all sites, and these negative controls are critical for detecting contamination and informing the false positive probability (Goldberg et al., 2016). Future work should include separate negative controls at each stage of the eDNA sampling process to help identify sources of contamination when it occurs and to properly model the false positive probability.

Notably, our false positive probability does not include scenarios in which we detect nonviable organisms or larval individuals: these are true-positive detections of eDNA present at the sampled site. In a management context, molecular detection of larvae alone does not necessarily indicate a high probability of invasion. However, with an invasive species with high larval-dispersal potential, larval detection beyond the known invasion front has high value for management planning and can be used to prioritize areas for assessment and prospecting.

False negative detections similarly erode an assay's usefulness in eDNA work, as in every other sampling method (Goldberg et al., 2016; Hunter et al., 2019). PCR inhibition can mask even high eDNA copy numbers and thereby profoundly affects molecular detection estimates (Jane et al., 2015). For example, DNA extracted from turbid water often contains humic acid and tannin compounds, created through non-enzymatic decay of the organic material, and these compounds can inactivate DNA polymerase and inhibit the PCR amplification process, reducing PCR efficiency or causing PCR failure (Albers et al., 2013; Goldberg et al., 2016). No samples included in this analysis were substantially inhibited, but it remains important to test for inhibition to guard against an inflated false negative rate in any molecular assay.

Conclusion

Given the limited resources available to State and tribal government agencies charged with controlling invasive species, there is significant value in identifying and implementing

optimal invasive species management strategies. Applications of eDNA methods represent one of the most significant advances in invasive species surveillance in the recent decade, yet uncertainty inherent in eDNA sampling means managers are often hesitant to direct management actions based solely on molecular evidence. Although previous work identifies the potential for DNA-based methods to amplify the uncertainty already associated with invasive species risk assessment (Benke et al., 2007; Darling & Mahon, 2011; Sikder et al., 2006), here we demonstrate that eDNA increases certainty at data-limited locations, and we highlight scenarios under which eDNA sampling is most useful in the context of green crab management. The value of eDNA sampling at low species densities and data-limited areas has largely been discussed (Crookes et al., 2020; Suarez-Menendez et al., 2020; Villacorta-Rath et al., 2020), but here we provide a means to formally quantify this value.

The joint model aids eDNA data interpretation and contributes to a growing body of analyses providing frameworks for inferring confidence in patterns of eDNA detections (Furlan et al., 2016; Guillera-Arroita et al., 2017; Lahoz-Monfort et al., 2016). This approach also offers a means to combine eDNA and traditional monitoring methods to make more reliable inferences about data-limited sites and provides reassurance to managers and other stakeholders leery of adopting a new technology. While environmental DNA methods can support detection of invasive species at low abundances, improved statistical methods to interpret patterns of environmental DNA detections can empower informed management responses.

Acknowledgements

We would like to thank the three anonymous reviewers and the editors of *Ecological Applications* for their constructive feedback that improved the manuscript. This work was funded by a grant from Washington Sea Grant, University of Washington, pursuant to National Oceanic and Atmospheric Administration Award No. NA18OAR4170095. The views expressed herein are those of the authors and do not necessarily reflect the views of NOAA or any of its sub-agencies. The trapping data used in this study was the product of a huge effort conducted by Washington Sea Grant (WSG) Crab Team, WA Department of Fish and Wildlife (WDFW), U.S. Department of Fish and Wildlife (USFWS), Jamestown S'Klallam Tribe, and Lummi Nation. Allen Pleus (WDFW) and Chelsey Buffington (WDFW) provided valuable management support and advice. Alex Stote (WSG), Amy Linhart (WSG), and Bethany McKim (USFWS) provided eDNA sampling assistance, and Neil Harrington (Jamestown S'Klallam Tribe) provided valuable insight into the history of green crab in Sequim Bay. Dr. Eily Allan and Dr. Zachary Gold provided encouragement and helpful comments on manuscript drafts, and Dr. Emily Jacobs-Palmer provided helpful laboratory advice. Dr. Sarah Brown and Dr. Todd Seamons contributed to the study design and interpretation of results.

References

Abdi, H. (2010). Coefficient of Variation. In N. Salkind (Ed.), *Encyclopedia of Research Design* (Vol. 1, pp. 169–171). Sage. https://doi.org/10.1049/cp.2010.0161

Albers, C. N., Jensen, A., Baelum, J., & Jacobsen, C. S. (2013). Inhibition of DNA polymerases used in q-PCR by structurally different soil-derived humic substances. *Geomicrobiology Journal*, *30*, 675–681.

Altwegg, R., & Nichols, J. D. (2019). Occupancy models for citizen-science data. *Methods in Ecology and Evolution*, *10*(1), 8–21. https://doi.org/10.1111/2041-210X.13090

Anderson, L. W. J. (2005). California's reaction to Caulerpa taxifolia: A model for invasive species rapid response. *Biological Invasions*, *7*(6), 1003–1016. https://doi.org/10.1007/s10530-004-3123-z

Andruszkiewicz, E. A., Sassoubre, L. M., & Boehm, A. B. (2017). Persistence of marine fish environmental DNA and the influence of sunlight. *PLoS ONE*, *12*(9), 1–18. https://doi.org/10.1371/journal.pone.0185043

Barnes, M. A., & Turner, C. R. (2016). The ecology of environmental DNA and implications for conservation genetics. *Conservation Genetics*, *17*(1), 1–17. https://doi.org/10.1007/s10592-015-0775-4

Beauclerc, K., Wozney, K., Smith, C., & Wilson, C. (2019). Development of quantitative PCR primers and probes for environmental DNA detection of amphibians in Ontario. *Conservation Genetics Resources*, *11*, 43–46.

Behrens Yamada, S., & Hunt, C. (2000). The Arrival and Spread of the European green crab, Carcinus maenas in the Pacific Northwest. *Dreissena!*, *11*(2), 1–7.

752 Beng, K. C., & Corlett, R. T. (2020). Applications of environmental DNA (eDNA) in ecology
753 and conservation: Opportunities, challenges and prospects. In *Biodiversity and*
754 *Conservation* (Vol. 29, Issue 7, p. 2121). Springer Netherlands.
755 https://doi.org/10.1007/s10531-020-01980-0
756 Benke, K. K., Hamilton, A. J., & Lowell, K. E. (2007). Uncertainty analysis and risk assessment
757 in the management of environmental resources. *Australasian Journal of Environmental*
758 *Management*, *14*(4), 241–247. https://doi.org/10.1080/14486563.2007.9725173
759 Bergshoeff, J. A., McKenzie, C. H., & Favaro, B. (2019). Improving the efficiency of the Fukui
760 trap as a capture tool for the invasive European green crab (Carcinus maenas) in
761 Newfoundland, Canada. *PeerJ*, *7*, e6308.
762 Biggs, J., Ewald, N., Valentini, A., Gaboriaud, C., Dejean, T., Griffiths, R. A., Foster, J.,
763 Wilkinson, J. W., Arnell, A., Brotherton, P., Williams, P., & Dunn, F. (2015). Using
764 eDNA to develop a national citizen science-based monitoring programme for the great
765 crested newt (Triturus cristatus). *Biological Conservation*, *183*, 19–28.
766 https://doi.org/10.1016/j.biocon.2014.11.029
767 Bohmann, K., Evans, A., Gilbert, M. T. P., Carvalho, G. R., Creer, S., Knapp, M., Yu, D. W., &
768 de Bruyn, M. (2014). Environmental DNA for wildlife biology and biodiversity
769 monitoring. *Trends in Ecology and Evolution*, *29*(6), 358–367.
770 https://doi.org/10.1016/j.tree.2014.04.003
771 Carim, K. J., Bean, N. J., Connor, J. M., Baker, W. P., Jaeger, M., Ruggles, M. P., McKelvey, K.
772 S., Franklin, T. W., Young, M. K., & Schwartz, M. K. (2020). Environmental DNA
773 Sampling Informs Fish Eradication Efforts: Case Studies and Lessons Learned. *North*

American Journal of Fisheries Management, *40*(2), 488–508. https://doi.org/10.1002/nafm.10428

Carim, K. J., McKelvey, K. S., Young, M. K., Wilcox, T. M., & Schwartz, michael K. (2016). *A protocol for collecting environmental DNA samples from streams* (Gen. Tech. Rep. RMRS-GTR-355; p. 18 p.). U.S. Department of Agriculture, Forest Service, Rocky Mountain Research Station.

Carpenter, B., Gelman, A., Hoffman, M. D., Lee, D., Goodrich, B., Betancourt, M., Brubaker, M. A., Guo, J., Li, P., & Riddell, A. (2017). Stan: A probabilistic programming language. *Journal of Statistical Software*, *76*(1). https://doi.org/10.18637/jss.v076.i01

Chambert, T., Kendall, W. L., Hines, J. E., Nichols, J. D., Pedrini, P., Waddle, J. H., Tavecchia, G., Walls, S. C., & Tenan, S. (2015). Testing hypotheses on distribution shifts and changes in phenology of imperfectly detectable species. *Methods in Ecology and Evolution*, *6*(6), 638–647.

Crane, L. C., Goldstein, J. S., Thomas, D. W., Rexroth, K. S., & Watts, W. (2021). Effects of life stage on eDNA detection of the invasive European green crab (Carcinus maenas) in estuarine systems. *Ecological Indicators*, *124*, 107412–107412. https://doi.org/10.1016/j.ecolind.2021.107412

Cressie, N., Calder, C. A., Clark, J. S., Ver Hoef, J. M., & Wikle, C. K. (2009). Accounting for uncertainty in ecological analysis: The strengths and limitations of hierarchical statistical modeling. *Ecological Applications*, *19*(3), 553–570.

Cristescu, M. E., & Hebert, P. D. N. (2018). Uses and misuses of environmental DNA in biodiversity science and conservation. *Annual Review of Ecology, Evolution, and Systematics*, *49*, 209–230. https://doi.org/10.1146/annurev-ecolsys-110617-062306

Crookes, S., Heer, T., Castañeda, R. A., Mandrak, N. E., Heath, D. D., Weyl, O. L. F., MacIsaac, H. J., & Foxcroft, L. C. (2020). Monitoring the silver carp invasion in Africa: A case study using environmental DNA (eDNA) in dangerous watersheds. *NeoBiota*, *56*, 31–47.

Darling, J. A., Jerde, C. L., & Sepulveda, A. J. (2021). What do you mean by false positive? *Environmental DNA*, *3*, 879–883.

Darling, J. A., & Mahon, A. R. (2011). From molecules to management: Adopting DNA-based methods for monitoring biological invasions in aquatic environments. *Environmental Research*, *111*(7), 978–988. https://doi.org/10.1016/j.envres.2011.02.001

Darling, J., Jerde, C., & Sepulveda, A. (2021). What do you mean by false positive? *Environmental DNA*, *00*(1), 1–5.

Davison, P. I., Falcou-Préfol, M., Copp, G. H., Davies, G. D., Vilizzi, L., & Créach, V. (2019). Is it absent or is it present? Detection of a non-native fish to inform management decisions using a new highly-sensitive eDNA protocol. *Biological Invasions*, *21*(8), 2549–2560. https://doi.org/10.1007/s10530-019-01993-z

Deiner, K., & Altermatt, F. (2014). Transport distance of invertebrate environmental DNA in a natural river. *PLoS ONE*, *9*(2). https://doi.org/10.1371/journal.pone.0088786

Deiner, K., Bik, H. M., Mächler, E., Seymour, M., Lacoursière-Roussel, A., Altermatt, F., Creer, S., Bista, I., Lodge, D. M., de Vere, N., Pfrender, M. E., & Bernatchez, L. (2017). Environmental DNA metabarcoding: Transforming how we survey animal and plant communities. *Molecular Ecology*, *26*(21), 5872–5895. https://doi.org/10.1111/mec.14350

Ficetola, G. F., Miaud, C., Pompanon, F., & Taberlet, P. (2008). Species detection using environmental DNA from water samples. *Biology Letters*, *4*(4), 423–425. https://doi.org/10.1098/rsbl.2008.0118

820 Furlan, E. M., Gleeson, D., Hardy, C. M., & Duncan, R. P. (2016). A framework for estimating
821 the sensitivity of eDNA surveys. *Molecular Ecology Resources*, *16*(3), 641–654.
822 https://doi.org/10.1111/1755-0998.12483
823 Gabry, J., Stan Development Team, Andreae, M., Betancourt, M., Carpenter, B., Gao, Y.,
824 Gelman, A., Goodrich, B., Lee, D., Song, D., & Trangucci, R. (2018). *shinystan:*
825 *Interactive Visual and Numerical Diagnostics and Posterior Analysis for Bayesian*
826 *Models* (2.5.0) [R]. https://cran.r-project.org/web/packages/shinystan/index.html
827 Gallego, R., Jacobs-Palmer, E., Cribari, K., & Kelly, R. P. (2020). Environmental DNA
828 metabarcoding reveals winners and losers of global change in coastal waters.
829 *Proceedings of the Royal Society B: Biological Sciences*, *287*(1940), 20202424.
830 Glude, J. B. (1955). The effects of temperature and predators on the abundance of the soft-shell
831 clam, Mya arenaria, in New England. *Transactions of the American Fisheries Society*, *84*,
832 13–26.
833 Goldberg, C. S., Sepulveda, A., Ray, A., Baumgardt, J., & Waits, L. P. (2013). Environmental
834 DNA as a new method for early detection of New Zealand mudsnails (Potamopyrgus
835 antipodarum). *Freshwater Science*, *32*(3), 792–800. https://doi.org/10.1899/13-046.1
836 Goldberg, C. S., Turner, C. R., Deiner, K., Klymus, K. E., Thomsen, P. F., Murphy, M. A.,
837 Spear, S. F., McKee, A., Oyler-McCance, S. J., Cornman, R. S., Laramie, M. B., Mahon,
838 A. R., Lance, R. F., Pilliod, D. S., Strickler, K. M., Waits, L. P., Fremier, A. K.,
839 Takahara, T., Herder, J. E., & Taberlet, P. (2016). Critical considerations for the
840 application of environmental DNA methods to detect aquatic species. *Methods in*
841 *Ecology and Evolution*, *7*(11), 1299–1307. https://doi.org/10.1111/2041-210X.12595

Grason, E. W., McDonald, P. S., Adams, J., Litle, K., Apple, J. K., & Pleus, A. (2018). Citizen science program detects range expansion of the globally invasive European green crab in Washington State (USA). *Management of Biological Invasions*, *9*(1), 39–47. https://doi.org/10.3391/mbi.2018.9.1.04

Griffin, J. E., Matechou, E., Buxton, A. S., Bormpoudakis, D., & Griffiths, R. A. (2019). Modelling environmental DNA data; Bayesian variable selection accounting for false positive and false negative errors. *Journal of the Royal Statistical Society. Series C: Applied Statistics*, 377–392. https://doi.org/10.1111/rssc.12390

Guillera-Arroita, G., Lahoz-Monfort, J. J., van Rooyen, A. R., Weeks, A. R., & Tingley, R. (2017). Dealing with false-positive and false-negative errors about species occurrence at multiple levels. *Methods in Ecology and Evolution*, *8*(9), 1081–1091. https://doi.org/10.1111/2041-210X.12743

Guo, J., Gabry, J., Goodrich, B., & Weber, S. (2020). *Rstan* (2.12.2) [Computer software]. https://cran.r-project.org/web/packages/rstan/index.html

Harper, K. J., Anucha, N. P., Turnbull, J. F., Bean, C. W., & Leaver, M. J. (2018). Searching for a signal: Environmental DNA (eDNA) for the detection of invasive signal crayfish, pacifastacus leniusculus (Dana, 1852). *Management of Biological Invasions*, *9*(2), 137–148. https://doi.org/10.3391/mbi.2018.9.2.07

Hayes, K. R., Cannon, R., Neil, K., & Inglis, G. (2005). Sensitivity and cost considerations for the detection and eradication of marine pests in ports. *Marine Pollution Bulletin*, *50*(8), 823–834. https://doi.org/10.1016/j.marpolbul.2005.02.032

Hinlo, R., Gleeson, D., Lintermans, M., & Furlan, E. (2017). Methods to maximise recovery of environmental DNA from water samples. *PLoS ONE*, *12*(6), 1–22. https://doi.org/10.1371/journal.pone.0179251

Hobbs, N. T., & Hooten, M. B. (2015). *Bayesian Models: A Statistical Primer for Ecologists*. Princeton University Press.

Hunter, M. E., Ferrante, J. A., Meigs-Friend, G., & Ulmer, A. (2019). Improving eDNA yield and inhibitor reduction through increased water volumes and multi-filter isolation techniques. *Scientific Reports*, *9*(1), 1–9. https://doi.org/10.1038/s41598-019-40977-w

Hunter, M. E., Oyler-McCance, S. J., Dorazio, R. M., Fike, J. A., Smith, B. J., Hunter, C. T., Reed, R. N., & Hart, K. M. (2015). Environmental DNA (eDNA) sampling improves occurrence and detection estimates of invasive Burmese pythons. *PLoS ONE*, *10*(4), 1–17. https://doi.org/10.1371/journal.pone.0121655

Jamestown S'Klallam Tribe. (2007). *Protecting and restoring the Waters of the Dungeness* (CWA 319 Plan).

Jane, S. F., Wilcox, T. M., Mckelvey, K. S., Young, M. K., Schwartz, M. K., Lowe, W. H., Letcher, B. H., & Whiteley, A. R. (2015). Distance, flow and PCR inhibition: EDNA dynamics in two headwater streams. *Molecular Ecology Resources*, *15*(1), 216–227. https://doi.org/10.1111/1755-0998.12285

Jerde, C. L. (2019). Can we manage fisheries with the inherent uncertainty from eDNA? *Journal of Fish Biology*, *November 2019*, 341–353. https://doi.org/10.1111/jfb.14218

Jerde, C. L., Mahon, A. R., Chadderton, W. L., & Lodge, D. M. (2011). "Sight-unseen" detection of rare aquatic species using environmental DNA. *Conservation Letters*, *4*(2), 150–157. https://doi.org/10.1111/j.1755-263X.2010.00158.x

886 Jo, T., Ikeda, S., Fukuoka, A., Inagawa, T., Okitsu, J., Katano, I., Doi, H., Nakai, K., Ichiyanagi,
887 H., & Minamoto, T. (2021). Utility of environmental DNA analysis for effective
888 monitoring of invasive fish species in reservoirs. *Ecosphere*, *12*(6), e03643.
889 Kelly, R. P., Port, J. A., Yamahara, K. M., Martone, R. G., Lowell, N. C., Thomsen, P. F., Mach,
890 M. E., Bennett, M., Prahler, E., Caldwell, M. R., & Crowder, L. B. (2014). Harnessing
891 DNA to improve environmental management. *Science*, *344*(6191), 1455–1456.
892 Khalsa, N. S., Smith, J., Jochum, K. A., Savory, G., & López, J. A. (2020). Identifying Under-Ice
893 Overwintering Locations of Juvenile Chinook Salmon by Using Environmental DNA.
894 *North American Journal of Fisheries Management*, *40*(3), 762–772.
895 Kuehne, L. M., Ostberg, C. O., Chase, D. M., Duda, .J.J., & Olden, J. D. (2020). Use of
896 environmental DNA to detect the invasive aquatic plants Myriophyllum spicatum and
897 Egeria densa in lakes. *Freshwater Science*, *39*(3), 521–533.
898 Lacoursière-Roussel, A., & Deiner, K. (2021). Environmental DNA is not the tool by itself.
899 *Journal of Fish Biology*, *98*(2), 383–386. https://doi.org/10.1111/jfb.14177
900 Lahoz-Monfort, J. J., Guillera-Arroita, G., & Tingley, R. (2016). Statistical approaches to
901 account for false-positive errors in environmental DNA samples. *Molecular Ecology*
902 *Resources*, *16*(3), 673–685. https://doi.org/10.1111/1755-0998.12486
903 Larson, E. R., Graham, B. M., Achury, R., Coon, J. J., Daniels, M. K., Gambrell, D. K., Jonasen,
904 K. L., King, G. D., LaRacuente, N., Perrin-Stowe, T. I. N., Reed, E. M., Rice, C. J., Ruzi,
905 S. A., Thairu, M. W., Wilson, J. C., & Suarez, A. V. (2020). From eDNA to citizen
906 science: Emerging tools for the early detection of invasive species. *Frontiers in Ecology*
907 *and the Environment*, *18*(4), 194–202. https://doi.org/10.1002/fee.2162

908 Lele, S. R., & Dennis, B. (2009). Bayesian methods for hierarchical models: Are ecologists
909 making a Faustian bargain. *Ecological Applications*, *19*(3), 581–584.
910 Lele, S. R., Dennis, B., & Lutscher, F. (2007). Data cloning: Easy maximum likelihood
911 estimation for complex ecological models using Bayesian Markov chain Monte Carlo
912 methods. *Ecology Letters*, *10*, 551–563.
913 Lele, S. R., Moreno, M., & Bayne, E. (2012). Dealing with detection error in site occupancy
914 surveys: What can we do with a single survey? *Journal of Plant Ecology*, *5*(1), 22–31.
915 Lodge, D. M., Williams, S., MacIsaac, H. J., Hayes, K. R., Leung, B., Reichard, S., Mack, R. N.,
916 Moyle, P. B., Smith, M., Andow, D. A., Carlton, J. T., & McMichael, A. (2006).
917 Biological Invasions: Recommendations for U.S. Policy and Management. *Ecological*
918 *Applications*, *16*(6), 2035–2054.
919 Longmire, J., Maltbie, M., & Baker, R. J. (1997). Use of "lysis buffer" in DNA isolation and its
920 implications for museum collections. *Occasional Papers, Museum of Texas Tech*
921 *University*, *163*, 1–6.
922 MacKenzie, D. I., Nichols, J. D., Hines, J. E., Knutson, M. G., & Franklin, A. B. (2003).
923 Estimating site occupancy, colonization, and local extinction when a species is detected
924 imperfectly. *Ecology*, *84*, 2200–2207.
925 MacKenzie, D. I., Nichols, J. D., Lachman, G. B., Droege, S., Royle, J. A., & Langtimm, C. A.
926 (2002). Estimating site occupancy rates when detection probabilities are less than one.
927 *Ecology*, *83*, 2248–2255.
928 McClintock, B. T., Bailey, L. L., Pollock, K. H., & Simons, T. R. (2010). Unmodeled
929 observation error induces bias when inferring patterns and dynamics of species
930 occurrence via aural detections. *Ecology*, *91*(8), 2446–2454.

931 Mckelvey, K. S., Young, M. K., Knotek, W. L., Carim, K. J., Wilcox, T. M., Padgett-Stewart, T.
932 M., & Schwartz, M. K. (2016). Sampling large geographic areas for rare species using
933 environmental DNA: A study of bull trout Salvelinus confluentus occupancy in western
934 Montana. *Journal of Fish Biology*, *88*(3), 1215–1222. https://doi.org/10.1111/jfb.12863
935 Miller, D. A., Nichols, J. D., McClintock, B. T., Campbell Grant, E. H., Bailey, L. L., & Weir, L.
936 A. (2011). Improving occupancy estimation when two types of observational error occur:
937 Non-detection and species misidentification. *Ecology*, *92*(7), 1422–1428.
938 Mize, E. L., Erickson, R. A., Merkes, C. M., Berndt, N., Bockrath, K., Credico, J., Grueneis, N.,
939 Merry, J., Mosel, K., Tuttle-Lau, M., Von Ruden, K., Woiak, Z., Amberg, J. J.,
940 Baerwaldt, K., Finney, S., & Monroe, E. (2019). Refinement of eDNA as an early
941 monitoring tool at the landscape-level: Study design considerations. *Ecological*
942 *Applications*, *29*(6), e01951.
943 Morrison, S. A., Macdonald, N., Walker, K., Lozier, L., & Shaw, M. R. (2007). Facing the
944 dilemma at eradication's end: Uncertainty of absence and the Lazarus effect. *Frontiers in*
945 *Ecology and the Environment*, *5*, 271–276.
946 Natural England. (2017). *Wildlife Licensing Newsletter* [Technical Report].
947 O'Donnell, J. L., Kelly, R. P., Shelton, A. O., Samhouri, J. F., Lowell, N. C., & Williams, G. D.
948 (2017). Spatial distribution of environmental DNA in a nearshore marine habitat. *PeerJ*,
949 *2017*(2), 1–24. https://doi.org/10.7717/peerj.3044
950 Orzechowski, S. C. M., Frederick, P. C., Dorazio, R. M., & Hunter, M. E. (2019). Environmental
951 DNA sampling reveals high occupancy rates of invasive Burmese pythons at wading bird
952 breeding aggregations in the central Everglades. *PLoS ONE*, *14*, e0213943.

953 Pilliod, D. S., Goldberg, C. S., Arkle, R. S., & Waits, L. P. (2013). Estimating occupancy and
954 abundance of stream amphibians using environmental DNA from filtered water samples.
955 *Canadian Journal of Fisheries and Aquatic Sciences*, *70*(8), 1123–1130.
956 https://doi.org/10.1139/cjfas-2013-0047
957 R Development Core Team. (2021). *R: a language and environment for statistical computing*. R
958 Foundation for Statistical Computing. http://www.R-project.org
959 Renshaw, M. A., Olds, B. P., Jerde, C. L., McVeigh, M. M., & Lodge, D. M. (2015). The room
960 temperature preservation of filtered environmental DNA samples and assimilation into a
961 phenol—Chloroform—Isoamyl alcohol DNA extraction. *Molecular Ecology Resources*,
962 *15*(1), 168–176.
963 Rose, J. P., Wademan, C., Weir, S., Wood, J. S., & Todd, B. D. (2019). Traditional trapping
964 methods outperform eDNA sampling for introduced semi-aquatic snakes. *PLoS ONE*,
965 *14*(7), 1–17.
966 Roussel, J. M., Paillisson, J. M., Tréguier, A., & Petit, E. (2015). The downside of eDNA as a
967 survey tool in water bodies. *Journal of Applied Ecology*, *52*(4), 823–826.
968 https://doi.org/10.1111/1365-2664.12428
969 Roux, L. D., Giblot-Ducray, D., Bott, N. J., Wiltshire, K. H., Deveney, M. R., Westfall, K. M., &
970 Abbott, C. L. (2020). Analytical validation and field testing of a specific qPCR assay for
971 environmental DNA detection of invasive European green crab (Carcinus maenas).
972 *Environmental DNA*, *December 2019*, 1–12. https://doi.org/10.1002/edn3.65
973 Royle, J.A., & Nichols, J. D. (2003). Estimating Abundance from Repeated Presence-Absence
974 Data or Point Counts. *Ecology*, *84*(3), 777–790.

Royle, J. A., & Dorazio, R. M. (2008). *Hierarchical Modeling and Inference in Ecology: The Analysis of Data from Populations, Metapopulations and Communities*. Academic Press.

Russell, J. C., Binnie, H. R., Oh, J., Anderson, D. P., & Samaniego-Herrera, A. (2017). Optimizing confirmation of invasive species eradication with rapid eradication assessment. *Journal of Applied Ecology*, *54*(1), 160–169.

Sansom, B. J., & Sassoubre, L. M. (2017). Environmental DNA (eDNA) Shedding and Decay Rates to Model Freshwater Mussel eDNA Transport in a River. *Environmental Science and Technology*, *51*(24), 14244–14253. https://doi.org/10.1021/acs.est.7b05199

Schmelzle, M. C., & Kinziger, A. P. (2016). Using occupancy modelling to compare environmental DNA to traditional field methods for regional-scale monitoring of an endangered aquatic species. *Molecular Ecology Resources*, *16*(4), 895–908. https://doi.org/10.1111/1755-0998.12501

Schmidt, B. R., Kéry, M., Ursenbacher, S., Hyman, O. J., & Collins, J. P. (2013). Site occupancy models in the analysis of environmental DNA presence/absence surveys: A case study of an emerging amphibian pathogen. *Methods in Ecology and Evolution*, *4*(7), 646–653. https://doi.org/10.1111/2041-210X.12052

Schütz, R., Tollrian, R., & Schweinsberg, M. (2020). A novel environmental DNA detection approach for the wading birds Platalea leucorodia, Recurvirostra avosetta and Tringa totanus. *Conservation Genetics Resources*, *Table 1*, 1–3. https://doi.org/10.1007/s12686-020-01143-x

Sepulveda, A. J., Hutchins, P. R., Forstchen, M., Mckeefry, M. N., & Swigris, A. M. (2020). The Elephant in the Lab (and Field): Contamination in Aquatic Environmental DNA Studies. *Frontiers in Ecology and Evolution*, *8*, 609973.

998 Sepulveda, A. J., Nelson, N. M., Jerde, C. L., & Luikart, G. (2020). Are Environmental DNA
999 Methods Ready for Aquatic Invasive Species Management? *Trends in Ecology and*
1000 *Evolution*, *35*(8), 668–678. https://doi.org/10.1016/j.tree.2020.03.011
1001 Sigsgaard, E. E., Carl, H., Møller, P. R., & Thomsen, P. F. (2015). Monitoring the near-extinct
1002 European Weather Loach in Denmark based on environmental DNA from water samples.
1003 *Biological Conservation*, *183*, 46–52.
1004 Sikder, I. U., Mal-Sarkar, S., & Mal, T. K. (2006). Knowledge-based risk assessment under
1005 uncertainty for species invasion. *Risk Analysis*, *26*(1), 239–252.
1006 Smart, A. S., Weeks, A. R., van Rooyen, A. R., Moore, A., McCarthy, M. A., & Tingley, R.
1007 (2016). Assessing the cost-efficiency of environmental DNA sampling. *Methods in*
1008 *Ecology and Evolution*, *7*(11), 1291–1298.
1009 Solymos, P. (2019). *dclone: Data Cloning and MCMC Tools for Maximum Likelihood Methods*
1010 (2.3-0) [R]. https://cran.r-project.org/web/packages/dclone/index.html
1011 Stratton, C., Sepulveda, A. J., & Hoegh, A. (2020). msocc: Fit and analyse computationally
1012 efficient multi-scale occupancy models in r. *Methods in Ecology and Evolution*, *11*(9),
1013 1113–1120.
1014 Suarez-Menendez, M., Planes, S., Garcia-Vazquez, E., & Ardura, A. (2020). Early Alert of
1015 Biological Risk in a Coastal Lagoon Through eDNA Metabarcoding. *Frontiers in*
1016 *Ecology and Evolution*, *8*(9).
1017 Tan, E. B. P., & Beal, B. F. (2015). Interactions between the invasive European green crab,
1018 Carcinus maenas (L.), and juveniles of the soft-shell clam, Mya arenaria L., in eastern
1019 Maine, USA. *Journal of Experimental Marine Biology and Ecology*, *462*, 62–73.

1020 Thomsen, P. F., & Willerslev, E. (2015). Environmental DNA - An emerging tool in
1021 conservation for monitoring past and present biodiversity. *Biological Conservation*,
1022 *183*(December), 4–18. https://doi.org/10.1016/j.biocon.2014.11.019
1023 Tucker, A. J., Chadderton, W. L., Jerde, C. L., Renshaw, M. A., Uy, K., Gantz, C., Mahon, A.
1024 R., Bowen, A., Strakosh, T., Bossenbroek, J. M., Sieracki, J. L., Beletsky, D., Bergner, J.,
1025 & Lodge, D. M. (2016). A sensitive environmental DNA (eDNA) assay leads to new
1026 insights on Ruffe (Gymnocephalus cernua) spread in North America. *Biological*
1027 *Invasions*, *18*(11), 3205–3222. https://doi.org/10.1007/s10530-016-1209-z
1028 Ulibarri, R. M., Bonar, S. A., Rees, C., Amberg, J., Ladell, B., & Jackson, C. (2017). Comparing
1029 Efficiency of American Fisheries Society Standard Snorkeling Techniques to
1030 Environmental DNA Sampling Techniques. *North American Journal of Fisheries*
1031 *Management*, *37*(3), 644–651.
1032 Vehtari, A., Gelman, A., & Gabry, J. (2017). Practical Bayesian model evaluation using leave-
1033 one-out cross-validation and WAIC. *Statistics and Computing*, *27*, 1413–1432.
1034 Villacorta-Rath, C., Adekunle, A. I., Edmunds, R. C., Strugnell, J. M., Schwarzkopf, L., &
1035 Burrows, D. (2020). Can environmental DNA be used to detect first arrivals of the cane
1036 toad, Rhinella marina, into novel locations? *Environmental DNA*, *2*(4), 635–646.
1037 Volkmann, H., Schwartz, T., Kirchen, S., Stofer, C., & Obst, U. (2007). Evaluation of inhibition
1038 and cross-reaction effects on real-time PCR applied to the total DNA of wastewater
1039 samples for the quantification of bacterial antibiotic resistance genes and taxon-specific
1040 targets. *Molecular and Cellular Probes*, *21*(2), 125–133.
1041 https://doi.org/10.1016/j.mcp.2006.08.009

Wimbush, J., Frischer, M. E., Zarzynski, J. W., & Nierzwicki-Bauer, S. A. (2009). Eradication of colonizing populations of zebra mussels (Dreissena polymorpha) by early detection and SCUBA removal: Lake George, NY. *Aquatic Conservation: Marine and Freshwater Ecosystems*, *19*(6), 703–713. https://doi.org/10.1002/aqc.1052

Woldt, A., McGovern, A., Lewis, T. D., & Tuttle-Lau, M. (2020). *Quality Assurance Project Plan: EDNA Monitoring of Bighead and Silver Carps* (pp. 1–91). U.S. Fish and Wildlife Service, USFWS Great Lakes Region 3.

Yoccoz, N. G. (2012). The future of environmental DNA in ecology. *Molecular Ecology*, *21*(8), 2031–2038. https://doi.org/10.1111/j.1365-294X.2012.05505.x

Tables

Table 1: Parameters estimated by the joint model, with the median and 90% credibility intervals (highest density interval calculation) of the 10,000 sampling iterations. Φ is the overdispersion parameter in the negative binomial distribution of species counts (*Eq. 1*), β is the coefficient relating species density to true positive molecular detection probability (*Eq. 2*), and p_{10} is the false positive molecular detection probability (*Eq. 3*).

Parameter	Median Estimate	90% Credibility Interval
Φ	0.94	0.72, 1.2
β	2.5	1.6, 3.5
p_{10}	0.022	0.0095, 0.048

Figures

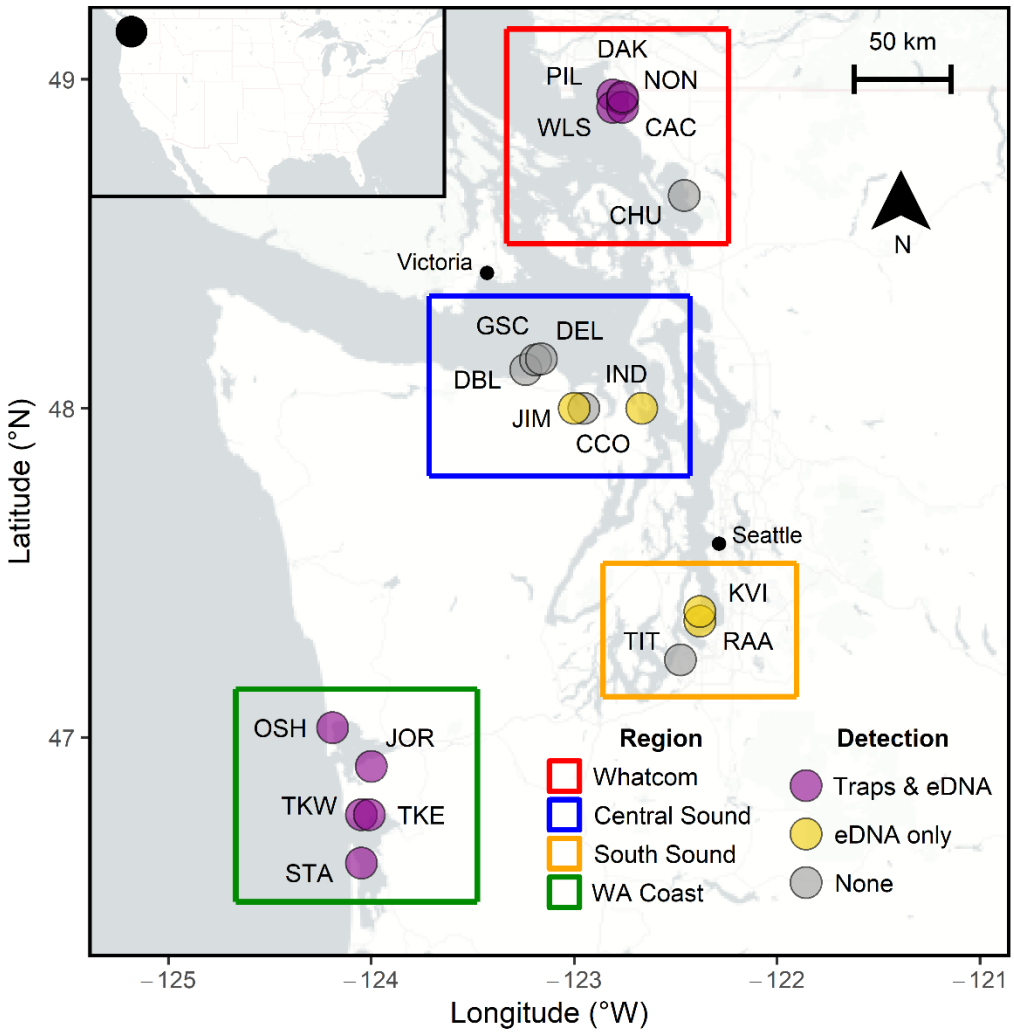

Figure 1: Environmental DNA and trapping detections of green crab over the sampling period. Purple dots indicate sites where green crabs were trapped and eDNA samples yielded at least one positive detection. Yellow dots indicate sites where no green crabs were trapped and eDNA samples yielded at least one positive detection. Grey dots indicate sites where no green crabs were trapped and eDNA samples yielded no positive detections. Sampled sites are labeled with site ID and polygons are colored by region. Inset map indicates study location in the context of the United States.

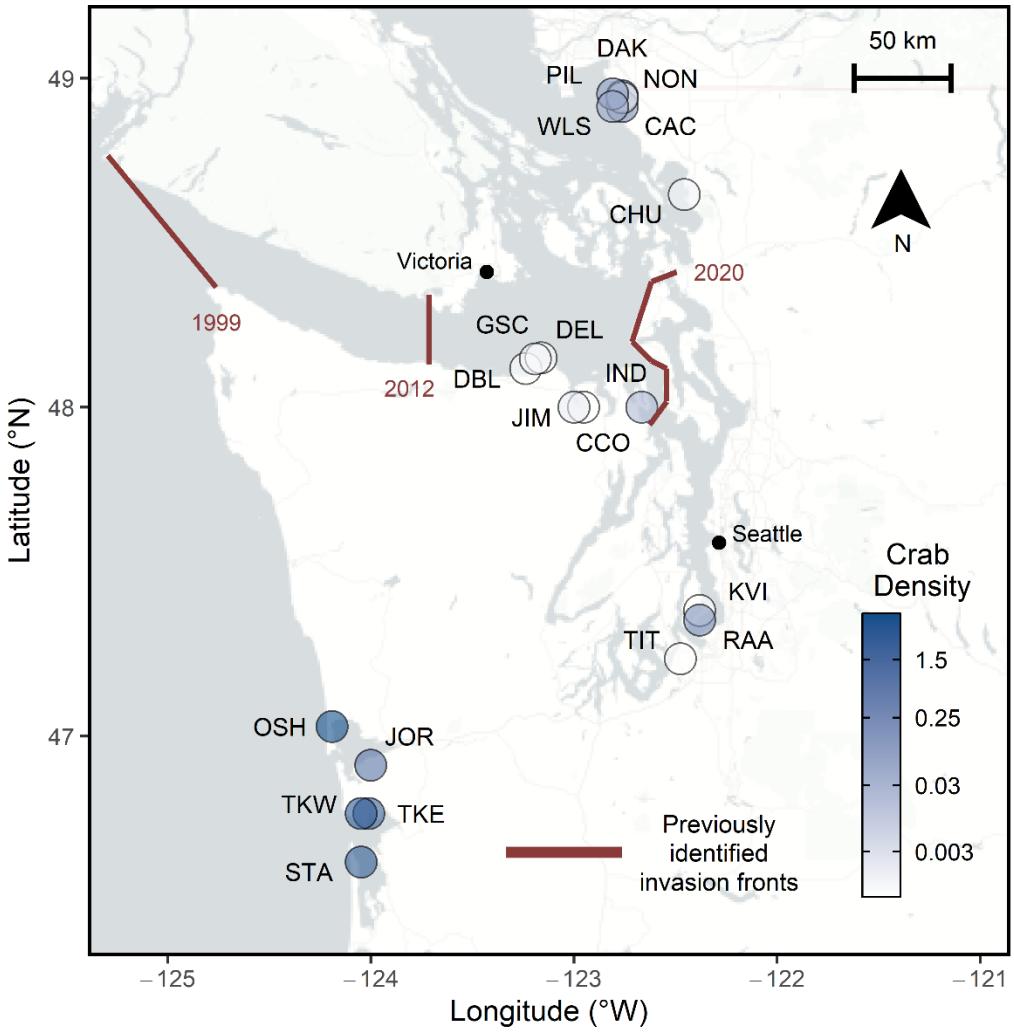

1094

1095 ***Figure 2***: Median of the joint model's posterior distributions of estimated green crab density at

1096 the 20 sampled sites. Colors indicate the median green crab density (crabs/trap) estimated by the

1097 joint model. The red lines designate previously identified invasion fronts in 1999, 2012, and

1098 2020.

1099

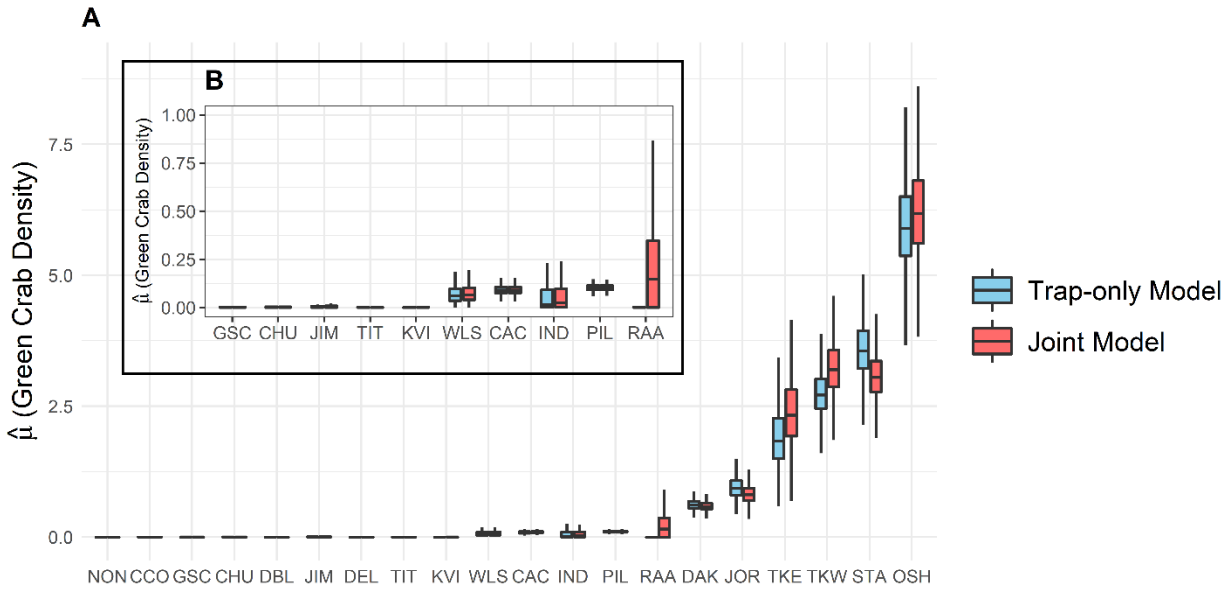

Figure 3A: Posterior distributions of estimated green crab density at each of the twenty sampled sites. Red boxplots are the estimated densities using the joint model, incorporating both trapping and eDNA information, and blue boxplots are the estimated densities using the trap-only model, using only trapping information. The lower and upper hinges correspond to the posterior data's first and third quartiles. ***B.*** Subset of sites where the joint model's estimated median green crab density ranges between 4.4e-8 and 0.1 crabs/trap.

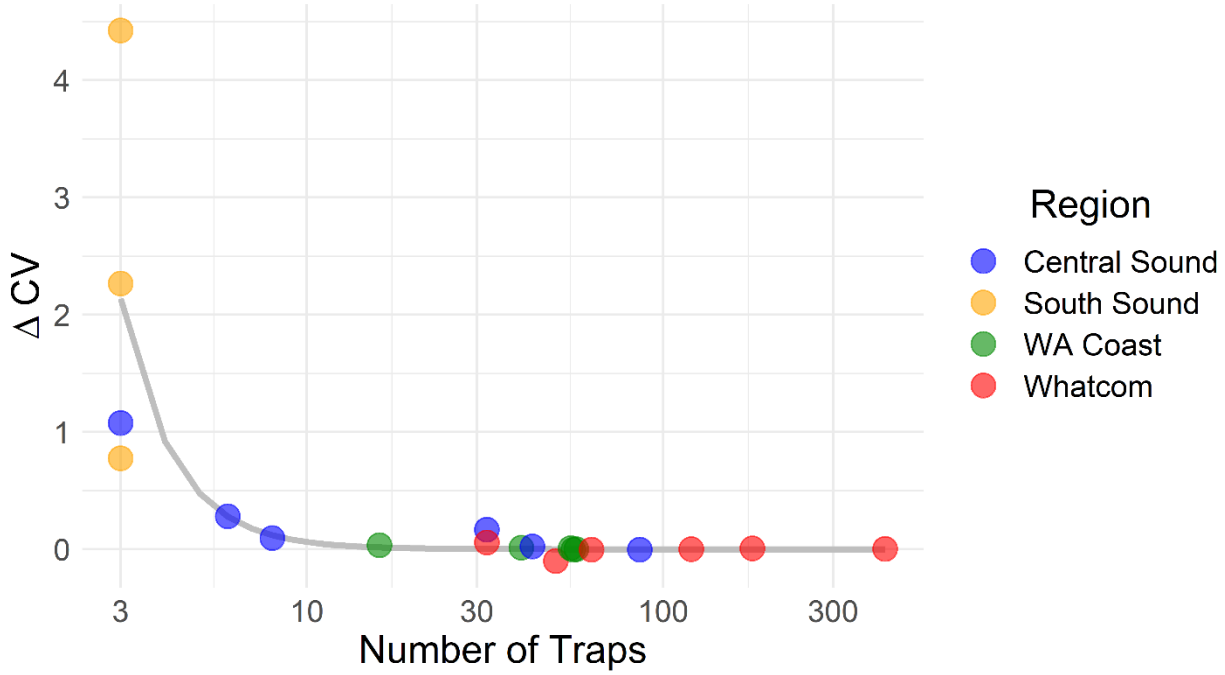

Figure 4: The difference in the coefficient of variation (ΔCV) in the posterior distributions of the estimated green crab densities between a model using only trapping information (trap-only model) and a model using both trapping and eDNA information (joint model). The gray line designates the best-fit trend line, ΔCV = 54*exp(-2.94*log(traps)).

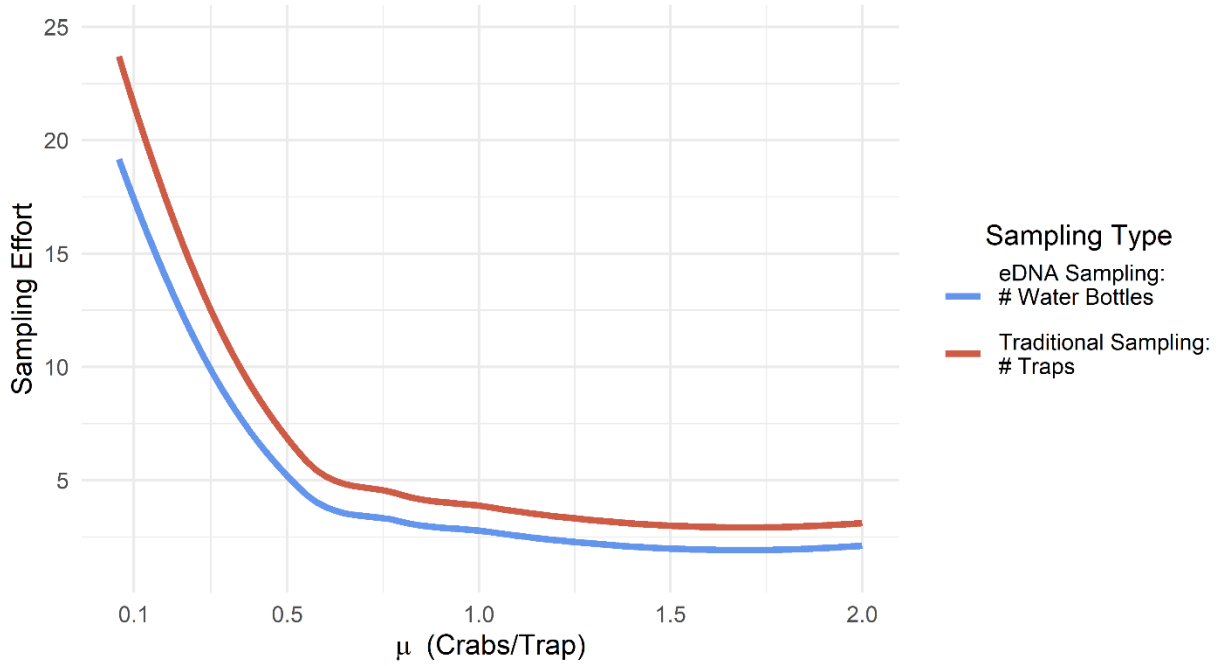

Figure 5: The sampling effort necessary to detect a green crab with 90% confidence. Lines designate the type of sampling effort (water bottles, traps).

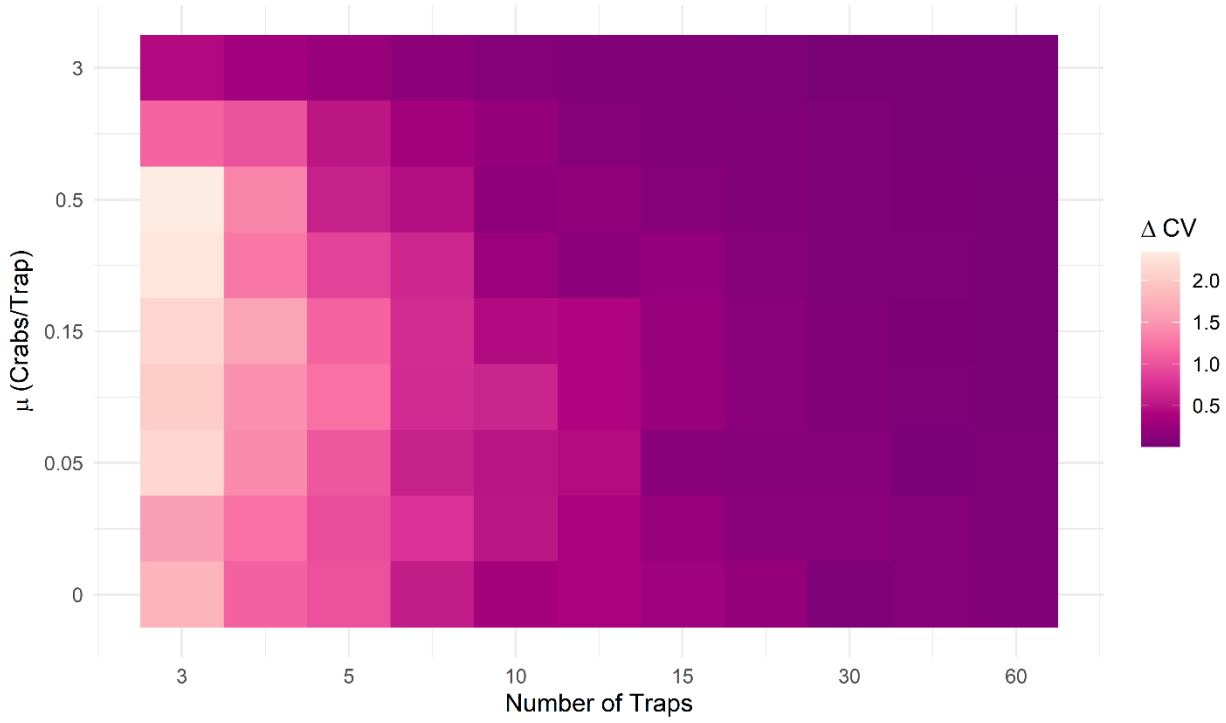

Figure 6: The marginal benefit of eDNA data at each simulated true crab density and trapping effort. The information benefit is represented by the difference in the coefficient of variation (ΔCV) in the posterior distributions of the estimated green crab densities between a model using only trapping information (trap-only model) and a model using both trapping and eDNA information (joint model). Each grid cell represents the mean ΔCV for all simulation scenario replicates. Note: Both the x and y axes are presented on a non-linear scale.

Tracking an invasion front with environmental DNA

Abigail G. Keller[1], Emily W. Grason[2], P. Sean McDonald[3], Ana Ramón-Laca[4], Ryan P. Kelly[1#]

Ecological Applications

Appendix S1

Methods

To evaluate the relative predictive accuracy of model choices that represent the green crab capturing process, we conducted a leave-one-out cross-validation (LOO) approach (Vehtari et al., 2017). Using the 'loo' package (version 2.4.1) (Vehtari et al., 2020), we estimated the pointwise out-of-sample prediction accuracy from two fitted models. The two models varied in the distribution choices used to represent the crab capture process in traps. *Eq. S1a* and *Eq. S1b* varied between models, and *Eq. S2-S4* were identical in the two models.

The observed count, Y, of a species at site *i* and trap sample *k* is drawn from a poisson distribution with a mean species density, μ_i (*Eq. S1a*).

$$Y_{i,k} \sim \text{Poisson}(\mu_i) \qquad \textit{Eq. S1a}$$

The observed count, Y, of a species at site *i* and trap sample *k* is drawn from a negative binomial distribution with a mean species density, μ_i, and an overdispersion parameter, Φ (*Eq. S1b*).

$$Y_{i,k} \sim \text{NegBinomial}(\mu_i, \Phi) \qquad \textit{Eq. S1b}$$

The relationship between the probability of a true molecular detection p_{11}, scaling coefficient β, and probability of a false molecular detection p_{10} remain the same as in the main manuscript (*Eq. S2-S4*).

$$p_{11,i} = \mu_i / (\mu_i + \beta) \quad \textit{Eq. S2}$$

$$p_i = p_{10} + p_{11,i} \quad \textit{Eq. S3}$$

$$K_{i,j} \sim \text{Binomial}(N_{i,j}, p_{i,}) \quad \textit{Eq. S4}$$

We ran the two models via 'rstan', with a step size of 0.5 and 4 chains with 500 warm-up and 2,500 sampling iterations per chain. The expected log pointwise predictive density (ELPD) was used to measure the goodness of the whole predictive distribution, and loo_compare() was used to compare the ELPD among the two models (Data S2).

Results

The model using a negative binomial distribution with an overdispersion parameter (*Eq. S1b*) provided the greatest predictive accuracy given the observed data (Table S1).

Table S1: Results of leave-one-out (LOO) cross-validation to compare the predictive accuracy of the model set. ELPD is the Bayesian LOO estimate of the expected log pointwise predictive density of the given model. SE is the standard error of the ELPD. ΔELPD is the difference between the model's ELPD and the ELPD of the model with the greatest predictive accuracy in the model set.

Model	Equation	ELPD	SE	ΔELPD
Negative binomial & overdispersion parameter	Eq. S1b	-856.8	42.3	-0.0
Poisson	Eq. S1a	-1023.6	66.9	-166.7

References

Vehtari, A., Gabry, J., Magnusson, M., Yao, Y., Bürkner, P.-C., Paananen, T., Gelman, A., Goodrich, B., Piironen, J., & Nicenboim, B. (2020). *loo: Efficient Leave-One-Out Cross-Validation and WAIC for Bayesian Models* (2.4.1) [R]. https://cran.r-project.org/web/packages/loo/index.html

Vehtari, A., Gelman, A., & Gabry, J. (2017). Practical Bayesian model evaluation using leave-one-out cross-validation and WAIC. *Statistics and Computing*, *27*, 1413–1432.

Tracking an invasion front with environmental DNA

Abigail G. Keller[1], Emily W. Grason[2], P. Sean McDonald[3], Ana Ramón-Laca[4], Ryan P. Kelly[1#]

Ecological Applications

Appendix S2

Due to the hierarchical qPCR data structure, where qPCR triplicates are nested within water bottles within sites, we provide a hierarchical version of the model that accounts for membership of qPCR replicates within nested groups. All molecular detection probabilities and species densities are estimated on a log scale. This model is suitable for datasets with sufficient intra-site and inter-site replication and was not implemented in the manuscript, since the dataset was not robust enough to estimate the variance in the probability of detection among bottles at a site, σ.

The observed count, Y, of a species at site *i* and trap sample *k* is drawn from a negative binomial distribution with a mean species density, μ_i, and an overdispersion parameter, Φ (*Eq. S1*).

$$Y_{i,k} \sim \text{NegBinomial}(\mu_i, \Phi) \qquad \textit{Eq. S1}$$

The probability of a true molecular detection, p_{11}, at site, *i*, is a saturating function of species density μ_i and scaling coefficient β (*Eq. S2*).

$$p_{11,i} = \mu_i / (\mu_i + \beta) \qquad \textit{Eq. S2}$$

The false positive probability, p_{10}, contributes to the overall molecular detection probability, p, at site *i* (*Eq. S3*; p is bounded between 0 and 1).

$$p_i = p_{10} + p_{11,i} \quad \textit{Eq. S3}$$

The probability of molecular detection, p, at site *i* and water sample *j* is drawn from a normal distribution with mean molecular detection probability, p, at site *i*, and a standard deviation, σ.

$$p_{j,i} \sim \text{Normal}(p_i, \sigma) \quad \textit{Eq. S4}$$

The number of positive qPCR detections, K, out of the number of trials, N, in water sample *j* at site *i* is drawn from a binomial distribution, with a probability of success on a single trial, p, at site *i* and water sample *j* (*Eq. S5*).

$$K_{i,j} \sim \text{Binomial}(N_{i,j}, p_{i,j}) \quad \textit{Eq. S5}$$

Tracking an invasion front with environmental DNA

Abigail G. Keller[1], Emily W. Grason[2], P. Sean McDonald[3], Ana Ramón-Laca[4], Ryan P. Kelly[1#]

Ecological Applications

Appendix S3

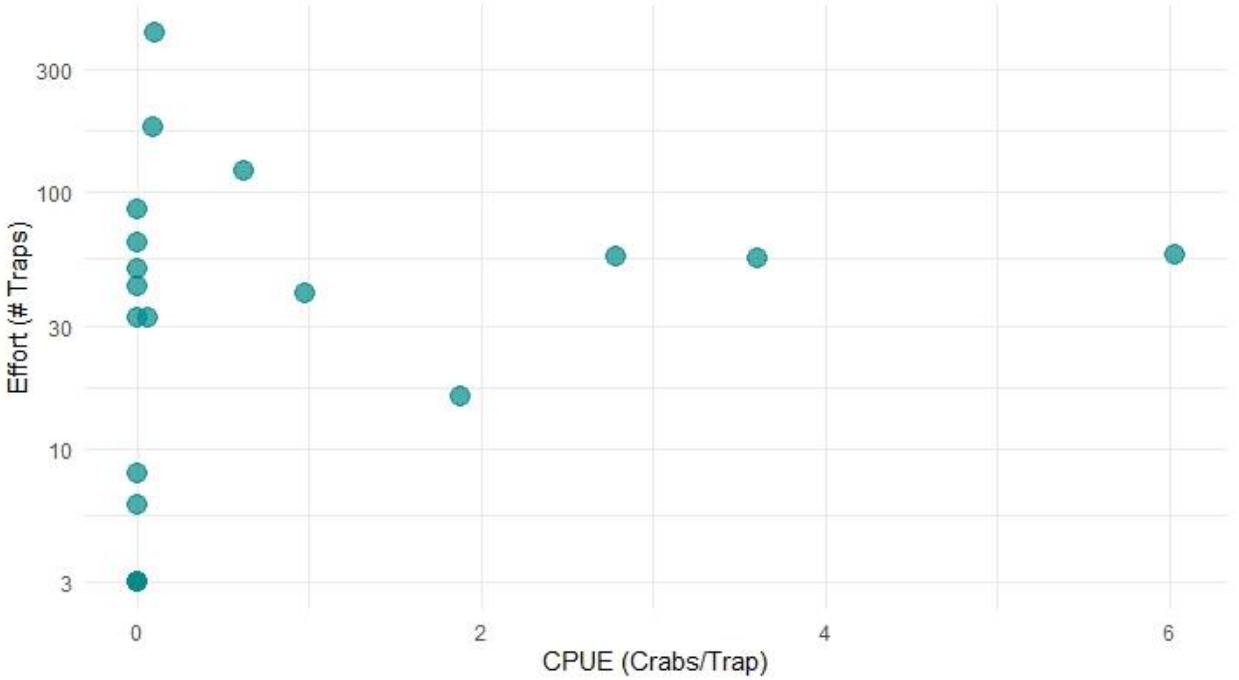

Figure S1: Depiction of trapping effort (number of traps) and green crab catch per unit effort (CPUE, crabs/trap) from 20 sampled sites over selected sampling period.

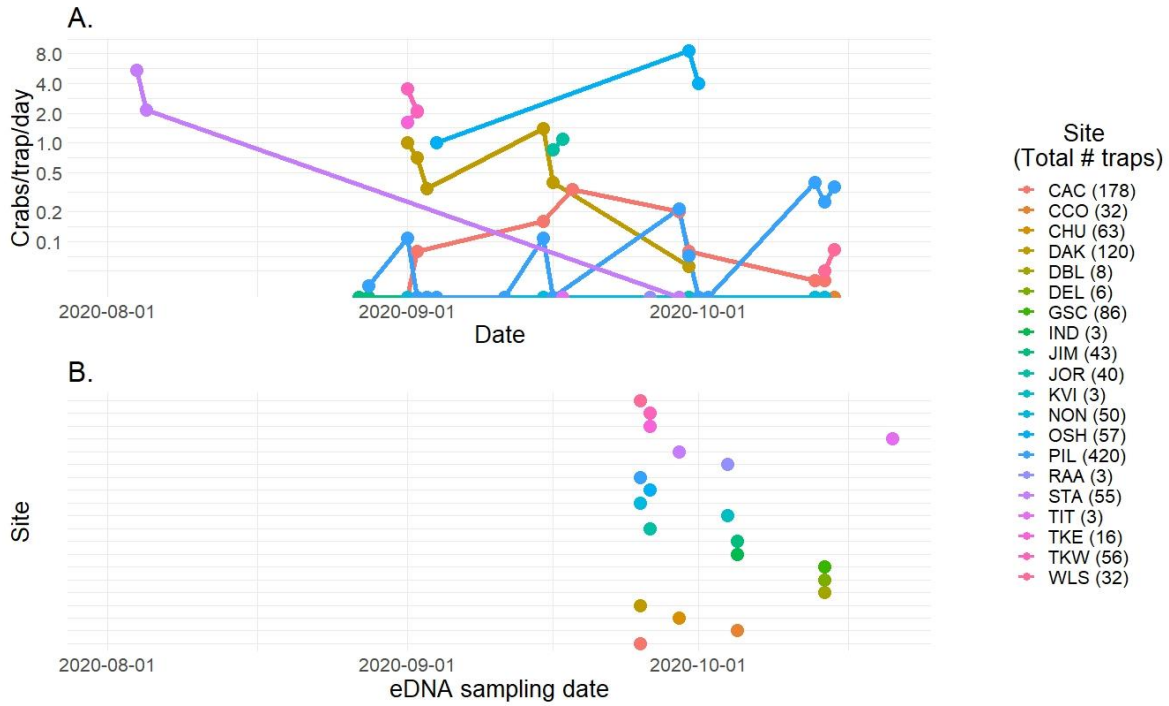

Figure S2: A. Number of crabs trapped per trap, per day at each of 20 sites over the designated sampling period. (Note: The 2020-09-29 date at the STA site represents only 3 traps). ***B.*** Date of eDNA sampling during sampling period.

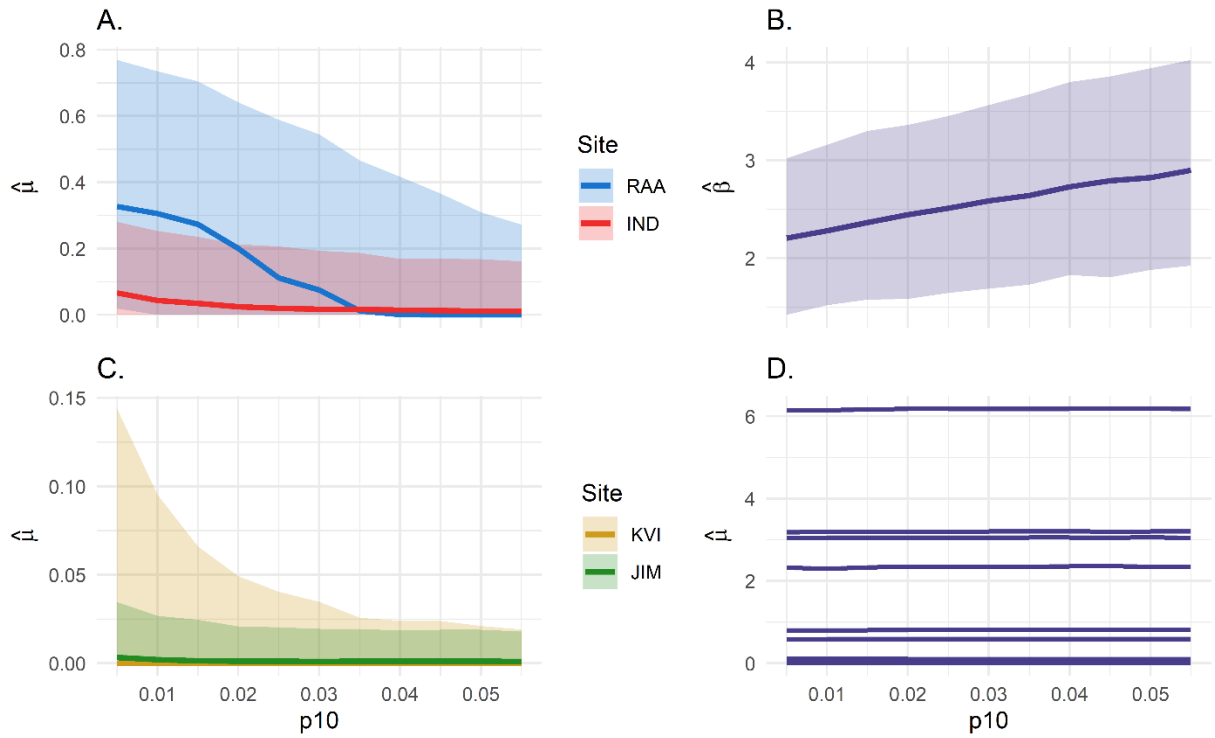

Figure S3: Results of sensitivity analysis used to assess sensitivity of the model's inferences to the specification of the false positive probability, p_{10}, prior distribution. Values on the x axis indicate the p10 value set prior to model refitting. ***A.*** Estimated μ for sites RAA and IND. Solid line indicates posterior median, and shaded area represents the 90% credibility interval. ***B.*** Solid line indicates posterior median for parameter β, and shaded area represents the 90% credibility interval. ***C.*** Estimated μ for sites KVI and JIM. Solid line indicates posterior median, and shaded area represents the 90% credibility interval. ***D.*** Estimated μ for sites KVI and JIM for remaining sites. Solid lines indicate posterior median.

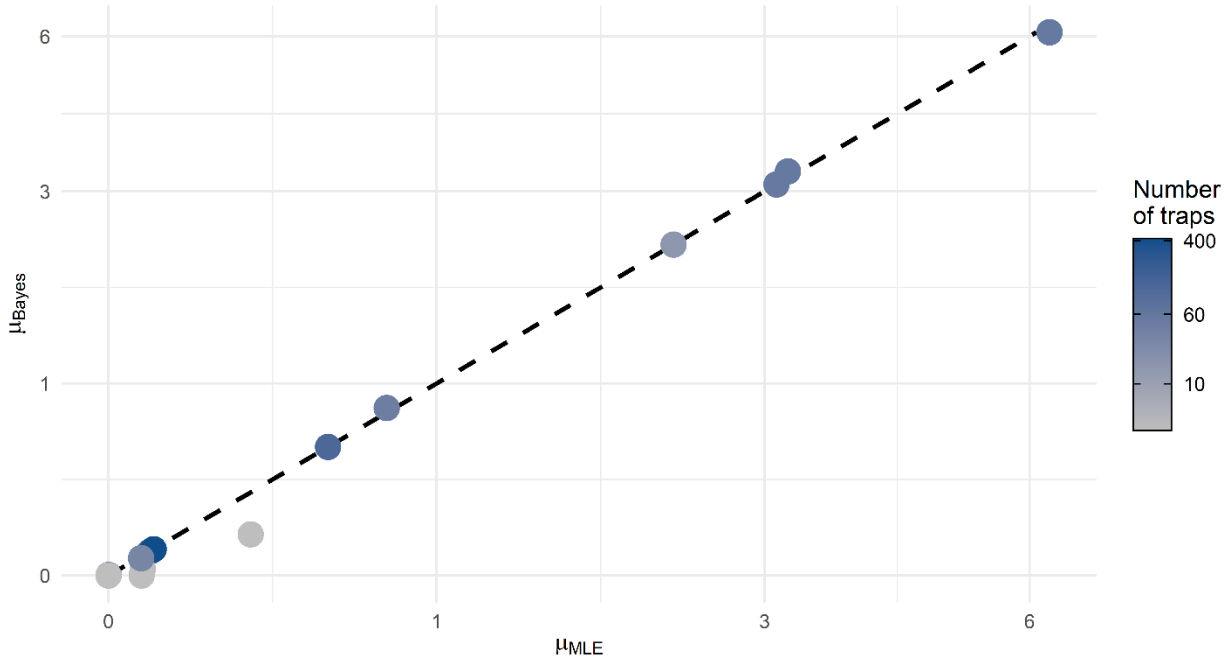

Figure S4: Comparison of parameter estimates of μ between the data cloning procedure (μ_{MLE}) and Bayesian model fitting (μ_{Bayes}). Points are colored by trapping effort at each site, and the dashed line represents the 1:1 line.

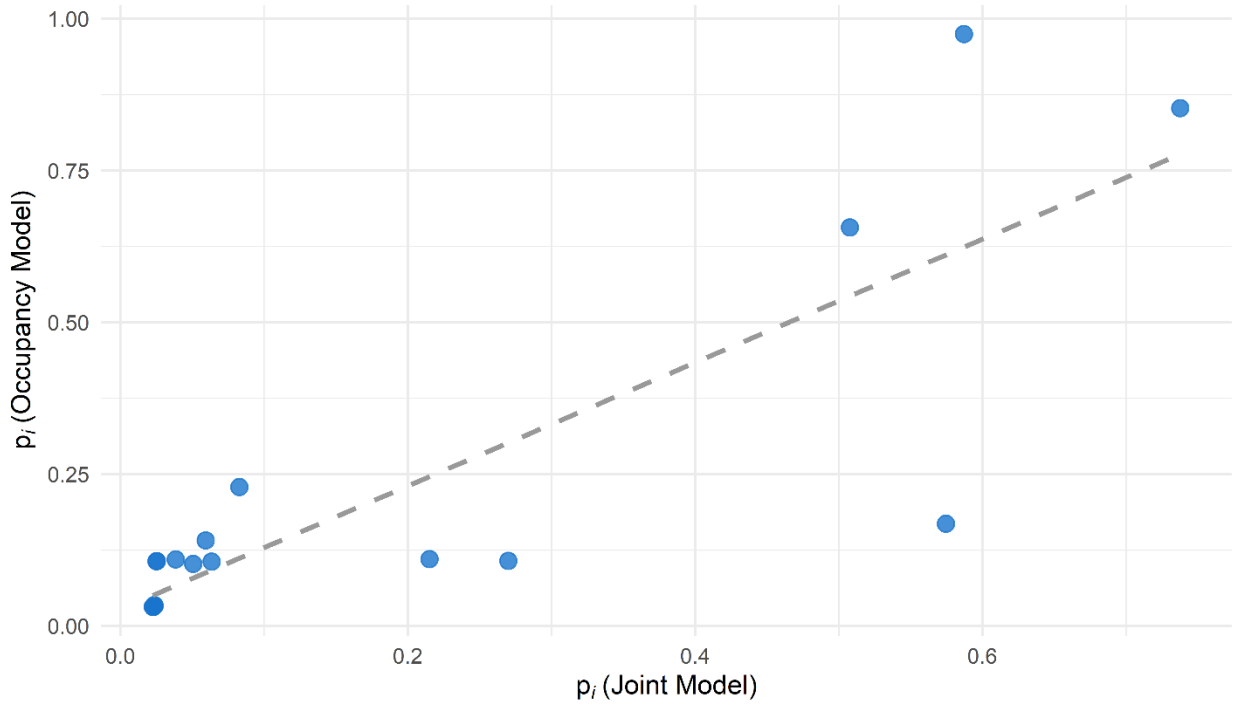

Figure S5: Comparison of parameter estimates of p_i (probability of molecular detection; p_{10} + p_{11}) at each site from the joint model and parameter estimates of p_i (replicate level occupancy probability) from an occupancy model framework. Dotted gray line indicates the fitted linear regression ($p_{i,occupancy} = 1.02*p_{i,joint} + 0.027$).

Tracking an invasion front with environmental DNA

Abigail G. Keller[1], Emily W. Grason[2], P. Sean McDonald[3], Ana Ramón-Laca[4], Ryan P. Kelly[1#]

Ecological Applications

Appendix S4

Table S1: Sanger sequencing results with the forward primer of the CO1 region. Note: Environmental samples from Lummi Sea Pond (LSP) were identically processed with other samples in this study, but the site was removed from modeling analysis due to insufficient trapping information.

Site	Region	Sample ID	Sequence
Lummi Sea Pond (LSP)	Central Sound	LSP-20201008-3	CNNGNGCTTCNGTTGATTTAGGGATTTTCTCTTTACATTTAGCCGGGGTTTCTTCTATTTTAGGAGCTGTAAATTTTATAACAACTATTATCAATATGCGTTCTNNC
Lummi Sea Pond (LSP)	Central Sound	LSP-20201008-4	CCNNNNNGGNGCTTCNGTTGATTTAGGGATTTTCTCTTTACATTTAGCCGGGGTTTCTTCTATTTTAGGAGCTGTAAATTTTATAACAACTATTATCAATATGCGTTCT
Ocean Shores (OSH)	Washington Coast	OSH-20200926-1	CCATNNNGGNGCTTCAGTTGANTTAGGGATTTTCTCTTTACATTTAGCCGGGGTTTCTTCTATTTTAGGAGCTGTAAATTTTATAACAACTATTATCAATATGCGTTCTTTC
Ocean Shores (OSH)	Washington Coast	OSH-20200926-2	CNGGNGCTTNNGTTGATTTAGGGATTTTCTCTTTACATTTAGCCGGGGTTTCTTCTATTTTAGGAGCTGTAAATTTTATAACAACTATTATCAATATGCGTTCTNNN
Ocean Shores (OSH)	Washington Coast	OSH-20200926-4	GCTTNNGNNGNNTTAGGGANTTTCTCTTTACATTTAGCCGGGGTTTCTTCTATTTTAGGAGCTGTAAATTTTATAACAACTATTATCAATATGCGTTCTNT
Ocean Shores (OSH)	Washington Coast	OSH-20200926-5	GGNGCTTCNGTTGNNTTAGGGANTTTCTCTTTACATTTAGCCGGGGTTTCTTCTATTTTAGGAGCTGTAAATTTTATAACAACTATTATCAATATGCGTTCTTTCA
Tokeland East (TKE)	Washington Coast	TKE-20200926-1	TGGNGCTTCNGTTGNNTTAGGGATTTTCTCTTTACATTTAGCCGGGGTTTCTTCTATTTTAGGAGCTGTAAATTTTATAACAACTATTATCAATATGCGTTCTTTCA
Tokeland East (TKE)	Washington Coast	TKE-20200926-4	GGNGCTTNNGTTGANTTAGGGANTTTCTCTTTACATTTAGCCGGGGTTTCTTCTATTTTAGGAGCTGTAAATTTTATAACAACTATTATCAATATGCGTTCTTTCAN

Tokeland West (TKW)	Washington Coast	TKW-20200926-1	TGGNGCTTCNGTTGNNTTAGGGATTTTCTCTTTACA TTTAGCCGGGGTTTCTTCTATTTTAGGAGCTGTAAA TTTTATAACAACTATTATCAATATGCGTTCTTTCA
Tokeland West (TKW)	Washington Coast	TKW-20200926-2	TGGNGCTTNNGTTGNNTTAGGGATTTTCTCTTTACA TTTAGCCGGGGTTTCTTCTATTTTAGGAGCTGTAAA TTTTATAACAACTATTATCAATATGCGTTCTTT
Tokeland West (TKW)	Washington Coast	TKW-20200926-3	CTGGNGCTTCAGTTGNNTTAGGGANTTTCTCTTTAC ATTTAGCCGGGGTTTCTTCTATTTTAGGAGCTGTAA ATTTTATAACAACTATTATCAATATGCGTTCTTTCA
Tokeland West (TKW)	Washington Coast	TKW-20200926-4	CNGGNGCTTCAGTTGANTTAGGGATTTTCTCTTTAC ATTTAGCCGGGGTTTCTTCTATTTTAGGAGCTGTAA ATTTTATAACAACTATTATCAATATGCGTTCTTTCA
Tokeland West (TKW)	Washington Coast	TKW-20200926-5	CNNTNNNTNNNNGNNNNNGTTGANTTAGGGANTTT CTCTTTACATTTAGCCGGGGTTTCTTCTATTTTAGG AGCTGTAAATTTTATAACAACTATTATCAATATGCG TTCTTTCA

1322
1323
1324
1325
1326
1327
1328
1329
1330
1331
1332
1333
1334
1335

1336 ***Table S2:*** Sites sampled for green crab eDNA. Sites within regions Central Sound, South Sound,
1337 Washington Coast, and Whatcom were used to construct the joint and trap-only models, and sites
1338 within Skagit Bay were used to inform the prior distribution for the probability of a false positive
1339 molecular detection, p_{10}. The hyperparameters for the prior distributions used to estimate μ at

each site are included, and these hyperparameters varied by sites with a history of trapped crabs from 2017-2020 (gamma(0.25, 0.25)) and sites without a history of trapped crabs from 2017-2020 (gamma(0.05, 0.05)).

Site (ID)	Date	Region	Latitude	Longitude	Hyper-parameters for μ gamma prior distribution
Chicken Coop Creek (CCO)	10/5/2020	Central Sound	48.02606	-122.99778	0.05, 0.05
Dungeness Base Lagoon (DBL)	10/14/2020	Central Sound	48.14652	-123.18392	0.05, 0.05
Dungeness East Lagoon (DEL)	10/14/2020	Central Sound	48.1766233	-123.1263022	0.05, 0.05
Graveyard Spit Channel (GSC)	10/14/2020	Central Sound	48.17371	-123.13612	0.25, 0.25
Indian Island (IND)	10/5/2020	Central Sound	48.02523	-122.71583	0.25, 0.25
Jimmycomelately Creek (JIM)	10/5/2020	Central Sound	48.02326	-123.00648	0.25, 0.25
KVI Beach (KVI)	10/4/2020	South Sound	47.42269	-122.43114	0.05, 0.05
Rabb's Lagoon (RAA)	10/4/2020	South Sound	47.39204	-122.43377	0.05, 0.05
Titlow (TIT)	10/21/2020	South Sound	47.24875	-122.55139	0.05, 0.05
John's River (JOR)	9/26/2020	Washington Coast	46.8997217	-123.9967067	0.25, 0.25
Ocean Shores (OSH)	9/26/2020	Washington Coast	46.99838	-124.13952	0.25, 0.25
Stackpole (STA)	9/29/2020	Washington Coast	46.59743	-124.03769	0.25, 0.25
Tokeland East (TKE)	9/26/2020	Washington Coast	46.70789	-123.97098	0.25, 0.25
Tokeland West (TKW)	9/26/2020	Washington Coast	46.70805	-123.97423	0.25, 0.25
California Creek (CAC)	9/25/2020	Whatcom	48.961843	-122.49613	0.25, 0.25
Chuckanut Creek (CHU)	9/29/2020	Whatcom	48.69919	-122.49613	0.25, 0.25
Dakota Creek (DAK)	9/25/2020	Whatcom	48.97244	-122.72922	0.25, 0.25
Noname Creek (NON)	9/25/2020	Whatcom	48.96821	-122.73333	0.05, 0.05
Pillars (PIL)	9/25/2020	Whatcom	48.989081	-122.754815	0.25, 0.25

Wilseis (WLS)	9/25/2020	Whatcom	48.989081	-122.754815	0.25, 0.25
Brown Point	2/21/2019	Skagit Bay	48.26974	-122.45904	N/A
Dugualla Bluff	2/21/2019	Skagit Bay	48.37722	-122.58163	N/A
Goat Island	2/21/2019	Skagit Bay	48.360889	-122.53468	N/A
Hoypus	2/21/2019	Skagit Bay	48.41127	-122.60754	N/A
Lone Tree Point	2/21/2019	Skagit Bay	48.40744	-122.55612	N/A
Mariners Bluff	2/21/2019	Skagit Bay	48.28214	-122.53178	N/A
Strawberry Point	2/21/2019	Skagit Bay	48.3214	-122.51651	N/A

Table S3: Quantitative PCR (qPCR) results of sampled sites. Five water samples were collected for 20 sites with trap data. DNA extracted from each water sample underwent three qPCR replicates, and the Ct is recorded for each replicate. Ct shift indicates the difference in Ct between the eDNA sample spiked with a synthetic positive control and the average of three positive controls.

Site (ID)	Region	Replicate 1	Replicate 2	Replicate 3	Ct Shift
Chicken Coop Creek (CCO)	Central Sound	No Ct	No Ct	No Ct	0.25
		No Ct	No Ct	No Ct	
		No Ct	No Ct	No Ct	
		No Ct	No Ct	No Ct	
		No Ct	No Ct	No Ct	
Dungeness Base Lagoon (DBL)	Central Sound	No Ct	No Ct	No Ct	-0.46
		No Ct	No Ct	No Ct	
		No Ct	No Ct	No Ct	
		No Ct	No Ct	No Ct	
		No Ct	No Ct	No Ct	
Dungeness East Lagoon (DEL)	Central Sound	No Ct	No Ct	No Ct	1.27
		No Ct	No Ct	No Ct	
		No Ct	No Ct	No Ct	
		No Ct	No Ct	No Ct	
		No Ct	No Ct	No Ct	
Graveyard Spit Channel (GSC)	Central Sound	No Ct	No Ct	No Ct	0.44
		No Ct	No Ct	No Ct	
		No Ct	No Ct	No Ct	
		No Ct	No Ct	No Ct	
		No Ct	No Ct	No Ct	
Indian Island (IND)	Central Sound	37.12	No Ct	No Ct	N/A
		No Ct	No Ct	No Ct	-0.09
		No Ct	No Ct	No Ct	-0.24
		No Ct	No Ct	No Ct	0.35
		No Ct	No Ct	No Ct	-0.49
Jimmycome-lately Creek (JIM)	Central Sound	No Ct	No Ct	No Ct	-0.81
		No Ct	37.46	No Ct	
		No Ct	No Ct	No Ct	
		No Ct	No Ct	No Ct	
		No Ct	No Ct	No Ct	
KVI Beach (KVI)	South Sound	No Ct	No Ct	No Ct	-0.3
		No Ct	No Ct	No Ct	0.6
		36.88	No Ct	No Ct	N/A
		No Ct	No Ct	No Ct	-0.52
		No Ct	No Ct	No Ct	1.64
	South Sound	No Ct	34.56	No Ct	N/A
		No Ct	36.76	No Ct	N/A

Rabb's Lagoon (RAA)		No Ct	No Ct	No Ct	-0.51
		No Ct	No Ct	No Ct	-1.04
		36.81	No Ct	No Ct	N/A
Titlow (TIT)	South Sound	No Ct	No Ct	No Ct	-0.12
		No Ct	No Ct	No Ct	
		No Ct	No Ct	No Ct	
		No Ct	No Ct	No Ct	
		No Ct	No Ct	No Ct	
John's River (JOR)	Washington Coast	No Ct	No Ct	36.82	N/A
		No Ct	No Ct	No Ct	1.28
		No Ct	No Ct	No Ct	1.41
		No Ct	No Ct	No Ct	0.42
		No Ct	No Ct	No Ct	0.07
Ocean Shores (OSH)	Washington Coast	36.42	34.54	34.47	N/A
		34.33	No Ct	37.29	
		38.5	37.1	37.67	
		36.25	34.16	33.64	
		34.82	34.25	34.43	
Stackpole (STA)	Washington Coast	No Ct	No Ct	No Ct	1.99
		No Ct	No Ct	No Ct	
		No Ct	37.08	No Ct	
		No Ct	No Ct	No Ct	
		No Ct	No Ct	36.41	
Tokeland East (TKE)	Washington Coast	36.15	35.59	No Ct	N/A
		36.25	36.23	34.45	
		No Ct	No Ct	36.35	
		35.45	35.23	34.66	
		No Ct	No Ct	35.15	
Tokeland West (TKW)	Washington Coast	33.75	33.24	33.69	N/A
		32.56	33.09	32.62	
		32.56	33.42	32.49	
		33.53	33.89	30.2	
		33.83	33.82	33.53	
California Creek (CAC)	Whatcom	No Ct	No Ct	No Ct	0.05
		No Ct	37.05	No Ct	N/A
		No Ct	No Ct	No Ct	0.82
		No Ct	No Ct	No Ct	-1.31
		No Ct	No Ct	No Ct	-0.91
	Whatcom	No Ct	No Ct	No Ct	-0.36

Chuckanut Creek (CHU)		No Ct	No Ct	No Ct	
		No Ct	No Ct	No Ct	
		No Ct	No Ct	No Ct	
		No Ct	No Ct	No Ct	
Dakota Creek (DAK)	Whatcom	No Ct	No Ct	No Ct	1
		No Ct	No Ct	No Ct	1.34
		No Ct	No Ct	37.73	N/A
		No Ct	No Ct	No Ct	-0.04
		No Ct	No Ct	No Ct	-0.3
Noname Creek (NON)	Whatcom	No Ct	No Ct	No Ct	
		No Ct	No Ct	No Ct	
		No Ct	No Ct	No Ct	0.25
		No Ct	No Ct	No Ct	
		No Ct	No Ct	No Ct	
Pillars (PIL)	Whatcom	No Ct	No Ct	No Ct	0.24
		No Ct	No Ct	No Ct	0.21
		No Ct	No Ct	No Ct	0.7
		No Ct	No Ct	No Ct	1.27
		No Ct	No Ct	36.11	N/A
Wilseis (WLS)	Whatcom	No Ct	No Ct	No Ct	0.11
		No Ct	No Ct	No Ct	0.93
		No Ct	No Ct	No Ct	0.92
		No Ct	No Ct	No Ct	0.82
		No Ct	No Ct	36.28	N/A

Table S4: Estimated green crab density, $\hat{\mu}$, at sampled sites. Table includes the median and 90% credibility interval of the parameter's posterior distribution.

Site (ID)	Region	median $\hat{\mu}$	90% Credibility Interval	$P(\hat{\mu} > \mu_{critical})$
Chicken Coop Creek	Central Sound	1.7e-8	1.9e-85, 0.0019	0.0028

Dungeness Base Lagoon	Central Sound	3.1e-8	4.8e-74, 0.0057	0.017
Dungeness East Lagoon	Central Sound	3.7e-8	9.6e-91, 0.0062	0.022
Graveyard Spit Channel	Central Sound	4.9e-4	2.4e-18, 0.0079	5e-4
Indian Island	Central Sound	0.024	1.3e-17, 0.21	0.35
Jimmycomelately Creek	Central Sound	0.0013	7.7e-17, 0.022	0.017
KVI Beach	South Sound	6.5e-7	2.0e-72, 0.051	0.096
Rabb's Lagoon	South Sound	0.16	4.0e-61, 0.61	0.64
Titlow	South Sound	4.4e-8	4.4e-66, 0.0082	0.032
John's River	Washington Coast	0.83	0.54, 1.1	1.0
Ocean Shores	Washington Coast	6.1	4.8, 7.7	1.0
Stackpole	Washington Coast	3.1	2.4, 3.8	1.0
Tokeland East	Washington Coast	2.3	1.3, 3.5	1.0
Tokeland West	Washington Coast	3.3	2.4, 4.1	1.0
Chuckanut Creek	Whatcom	6.0e-4	2.6e-17, 0.01	0.0019
California Creek	Whatcom	0.090	0.055, 0.13	0.96
Dakota Creek	Whatcom	0.59	0.46, 0.73	1.0
Noname Creek	Whatcom	9.5e-9	3.4e-69, 0.0012	6e-4
Pillars	Whatcom	0.10	0.076, 0.13	1.0
Wilsei's	Whatcom	0.065	0.0066, 0.14	0.59

1395

1396